AD-A040 436 TRW DEFENSE AND SPACE SYSTEMS GROUP REDONDO BEACH CALIF F/G 9/5
ADVANCED SURFACE ACOUSTIC WAVE (SAW) OSCILLATOR INVESTIGATION.(U)
APR 77 N00123-76-C-0588
UNCLASSIFIED NL

| OF |
AD
A040436

END

DATE
FILMED
6-77

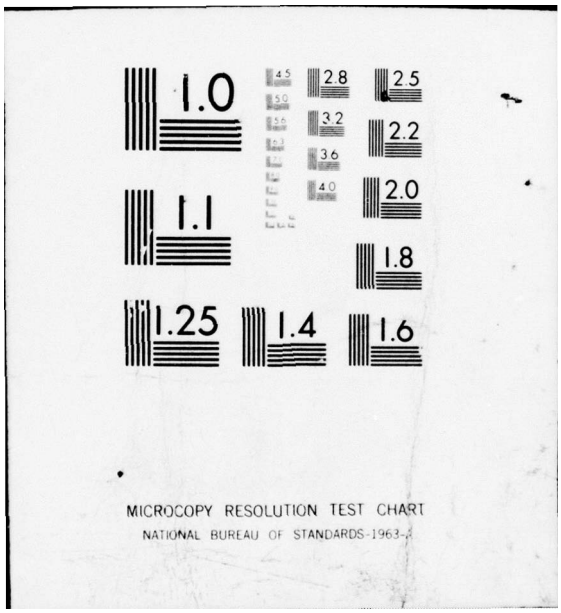
1.0
1.1
1.25
1.4
1.6
1.8
2.0
2.2
2.5
2.8
3.2
3.6
4.0
4.5
5.0
5.6
6.3
MICROCOPY RESOLUTION TEST CHART
NATIONAL BUREAU OF STANDARDS-1963-A

ADVANCED SURFACE ACOUSTIC WAVE (SAW) OSCILLATOR INVESTIGATION

April 1977

Contract No. N00123-76-C-0588

Prepared for
NAVAL OCEAN SYSTEMS CENTER
San Diego, California

By
TRW
DEFENSE AND SPACE SYSTEMS GROUP
ONE SPACE PARK • REDONDO BEACH, CALIFORNIA 90278

(6)

ADVANCED SURFACE ACOUSTIC WAVE (SAW) OSCILLATOR INVESTIGATION.

(9) Final rept. 1 Feb 76 - 1 Feb 77.

(12) 55p.

(11) April 1977

(15) Contract No. N00123-76-C-0588

Prepared for
NAVAL OCEAN SYSTEMS CENTER
San Diego, California

By

TRW
DEFENSE AND SPACE SYSTEMS GROUP
ONE SPACE PARK • REDONDO BEACH, CALIFORNIA 90278

409 637

LB

CONTENTS

ILLUSTRATIONS

ILLUSTRATIONS (Continued)

TABLES

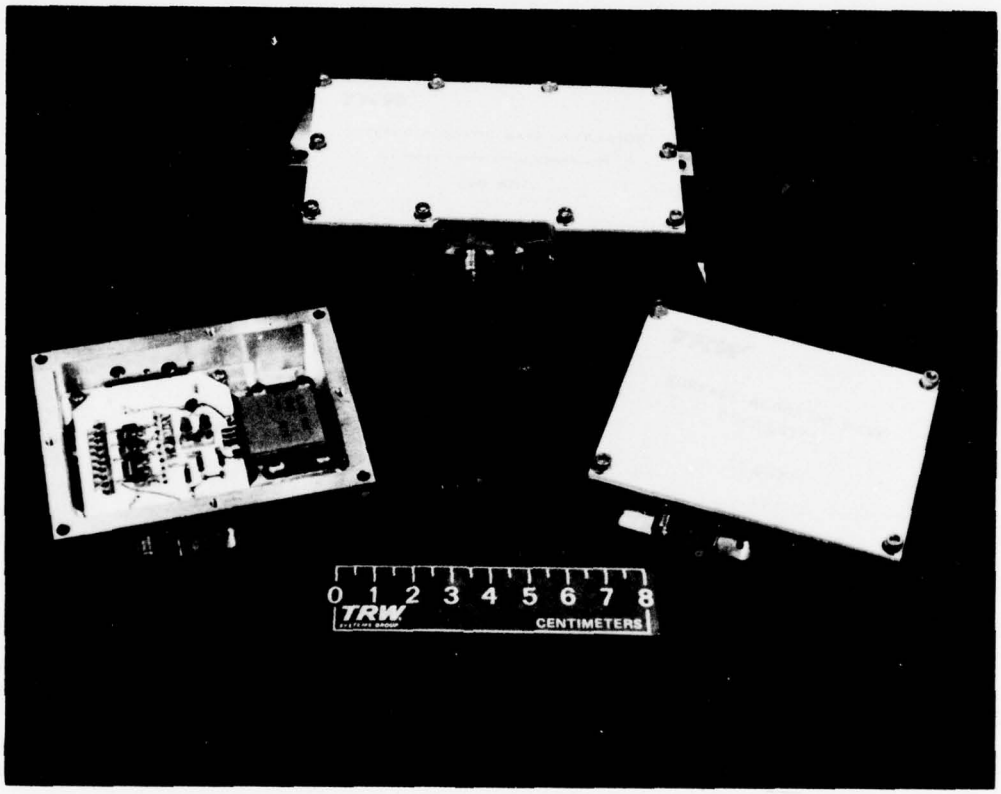
0 1 2 3 4 5 6 7 8
TRW
CENTIMETERS

1. INTRODUCTION

This final report describes the results of the development, fabrication, evaluation, and test performed by TRW Defense and Space Systems under Contract No. N00123-76-C-0588, Advanced Surface Acoustic Wave (SAW) Oscillator Investigation, for The Naval Ocean Systems Center. The period of performance was 1 February 1976 to 1 February 1977. The main purpose of the SAW oscillator program was the fabrication and characterization of SAW oscillators operating at 250 MHz, 500 MHz, and 1 GHz. As the data presented shows, the performance of these oscillators closely approaches or exceeds the current state-of-the-art in nearly every respect.

SAW oscillators offer several important advantages over bulk-effect crystal oscillators. Among these advantages, one of the most important is the higher fundamental frequency of oscillation. The SAW delay line which is the heart of the SAW oscillator can be fabricated to operate at frequencies in excess of 2 GHz. This inherently higher frequency of operation results in the elimination of costly multiplier chains, improved frequency source phase noise, and significant reductions in size, weight, and dc power. For these reasons, this program has focused on the fabrication and evaluation of advanced, state-of-the-art surface acoustic wave oscillators.

During the program, ten different SAW oscillators covering the frequency range of 225 MHz to 1.124 GHz were extensively characterized. The test results for two of these oscillators are particularly significant. The first oscillator operates at 250 MHz and employs a digital temperature compensation circuit. Using this technique, the overall temperature stability of the oscillator was improved by a factor of almost 10:1 over the basic stability of ST-cut quartz. The second important oscillator development was the design, fabrication, and characterization of a fundamental SAW oscillator operating at 1.124 GHz. This oscillator demonstrated state-of-the-art performance; particularly it exhibited phase noise which was comparable to the best bulk-oscillator/multiplier chain type sources.

As an additional task on this program, the SAW oscillator aging tests started on a previous contract were continued. A total of over 35,000 oscillator-hours of frequency aging data have been accumulated. Four 250 MHz SAW oscillators have been on continuous life test for over a year. The average frequency aging rate of the oscillators over the full year was -21 ppm per year. At the conclusion of these tests, the average frequency aging rate of the four oscillators had dropped to less than -5 ppm per year.

At the conclusion of the program, four SAW oscillators covering the frequency range of 250 MHz to 1.124 GHz were delivered to Naval Ocean Systems Center. In addition to the 250 MHz temperature compensated and the 1.124 GHz units previously described, one 250 MHz life test oscillator and a 500 MHz oscillator were delivered. Test and evaluation of these oscillators will be continued by NOSC.

2. SAW DELAY LINE DESIGN AND FABRICATION

This section describes the design and fabrication of the 1 GHz and temperature compensated SAW delay lines used in the oscillators described in Section 4. The 1 GHz SAW delay line was fabricated on ST-cut quartz utilizing conventional photolithographic techniques to achieve 0.7 μm transducer finger widths and spacing and represents a significant addition to the current SAW device state-of-the art. The temperature-compensated SAW delay line was fabricated on a composite structure of lithium tantalate ($LiTaO_3$) and silicon dioxide (SiO_2). The predicated behavior of the delay line temperature coefficient as a function of SiO_2 film thickness was confirmed and the SiO_2 film thickness necessary for a zero first order temperature coefficient was determined.

2.1 1 GHz SAW DELAY LINE

The 1 GHz SAW delay line was fabricated on ST-cut quartz utilizing conventional non-e-beam photolithographic techniques. Thin electrode transducers were employed for optimum delay line Q (and hence SAW oscillator short-term stability) consistent with the constraints set by the limitations of photomask generation. Figure 2-1 shows a typical thin electrode structure SAW delay line. This type of transducer has groups of electrodes, commonly referred to as sections, separated by large open areas. The advantage of a thin electrode transducer is that it allows the delay line to have good frequency selectivity (i.e., very narrow passband) with a relatively small number of fingers. This reduction of the number of fingers greatly minimizes delay line second order effects.

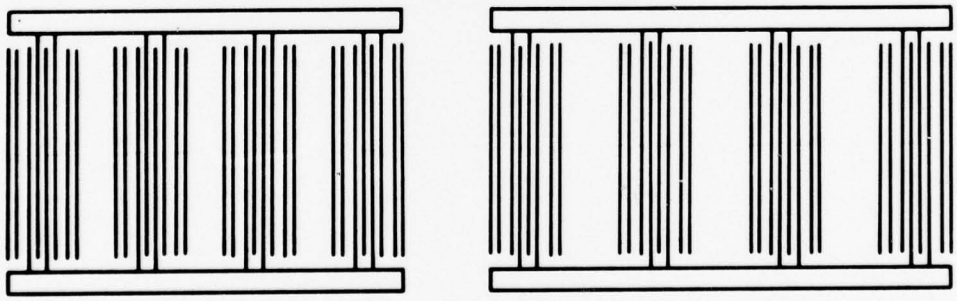

Figure 2-1. Thin Electrode Transducer Configuration

2.1.1 Saw Delay Line Design Considerations

Several factors which must be considered when designing high frequency SAW transducers. The most critical parameters fall into the general category of second order effects. These are effects due to the transducer metal film which only become significant when the SAW delay line frequency exceeds 500 MHz. Two physical mechanisms contribute to second order effects. The first mechanism is caused by the fact that

the tangential electric field is shorted out as the surface acoustic wave travels across the metal film. This results in a velocity change which produces both a slight shift in the center frequency of the transducer and an impedance discontinuity at the edge of the fingers. The second mechanism is caused by the added mass of the metallic film. This mass produces an impedance discontinuity at the edge of the fingers. These impedance discontinuities produce coherent multiple reflections which occur both within the transducer and between the transducers. These coherent multiple reflections manifest themselves in distortion of both amplitude and phase response.

Thin electrode transducers not only reduce the fingers or reflection points, but they have an added bonus. In the open areas between sections, one can place dummy, or unconnected, electrodes. Each section of the thin electrode transducer has a set of dummy electrodes which are offset from the active electrodes by one quarter wavelength. Since dummy electrodes have the same impedance discontinuity and are stepped out of phase with active electrodes, they produce a cancellation of reflections. The thin electrode transducers are designed such that there is an equal number of active and dummy electrodes on each section. Figure 2-2 shows this type of configuration.

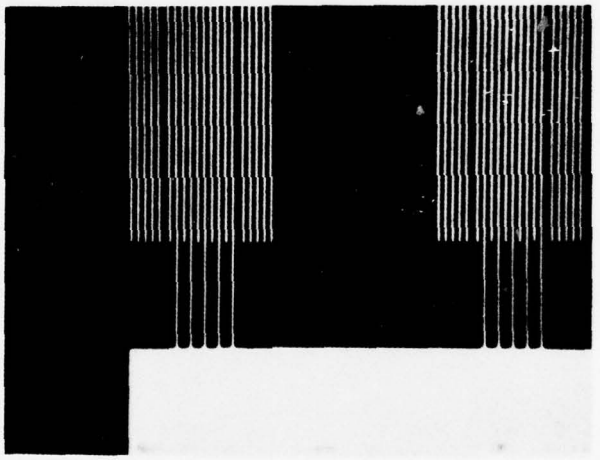

Figure 2-2. Transducer Configuration with Equal Number of Active and Dummy Electrodes

2.1.2 Computer Simulation of 1 GHz Transducer Patterns

Both a delta-function model and an equivalent circuit model were used to simulate the characteristic responses of the transducer patterns. The equivalent circuit approach was used to calculate the impedance characteristic and the minimum insertion loss of the transducer in the passband. The frequency response of the transducer was calculated using the delta function approach. The resultant transfer function, or response, of the SAW delay line is just the product of the individual transfer functions of the two transducers making up the delay line. These calculations were performed on the CDC Cyber 174 and Cyber 74 computers.

Thin electrode patterns were used for both the input and the output transducers of the 1 GHz SAW delay line. The frequency response of a thin electrode transducer is given as

$$H(f) \propto A \frac{\sin x}{x} \frac{\sin \hat{N}\pi f_o \tau_o}{\sin \pi f_o \tau_o} \qquad (2.1)$$

where

A = a constant related to material constants

$x = N\pi(f-f_o)/f_o$

N = number of finger pairs per section

$\hat{N}$ = number of sections

τ_o = time delay between sections

The frequency response for each of the transducers is shown in Figure 2-3. These curves were obtained by using the delta function approach to calculate their respective transfer functions. The response of the delay line is the product of the transfer function δ of the individual transducers. In order to suppress the sidelobes, the

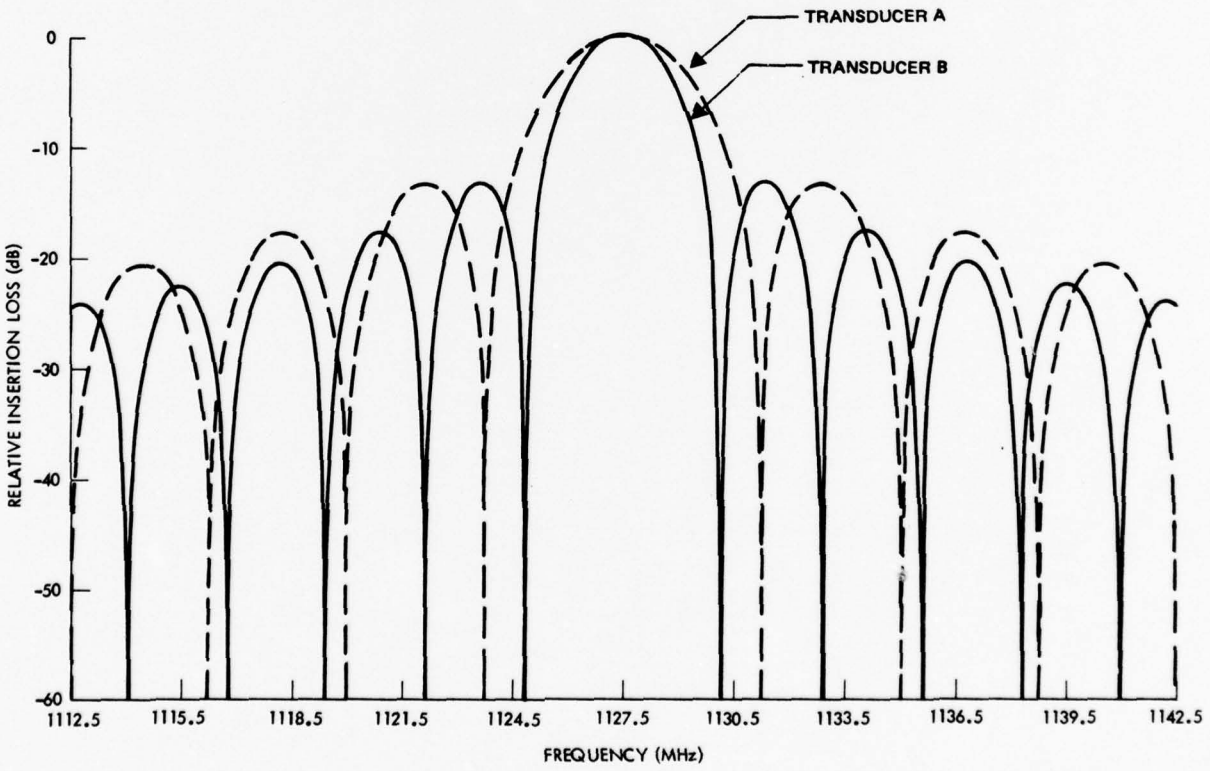

Figure 2-3. Individual Transducer Frequency Response

first minimum of the first transducer is made to lie at the maximum of the main sidelobe of the second transducer. The technique is clearly illustrated in Figure 2-4. The resultant frequency response is also shown in Figure 2-4. The center-to-center separation between transducers is adjusted so that the phase condition allows only one solution at the center of the passband. All other solutions are on nodal points. This minimizes the possibility of any frequency hopping or multimode generation occurring in the oscillator.

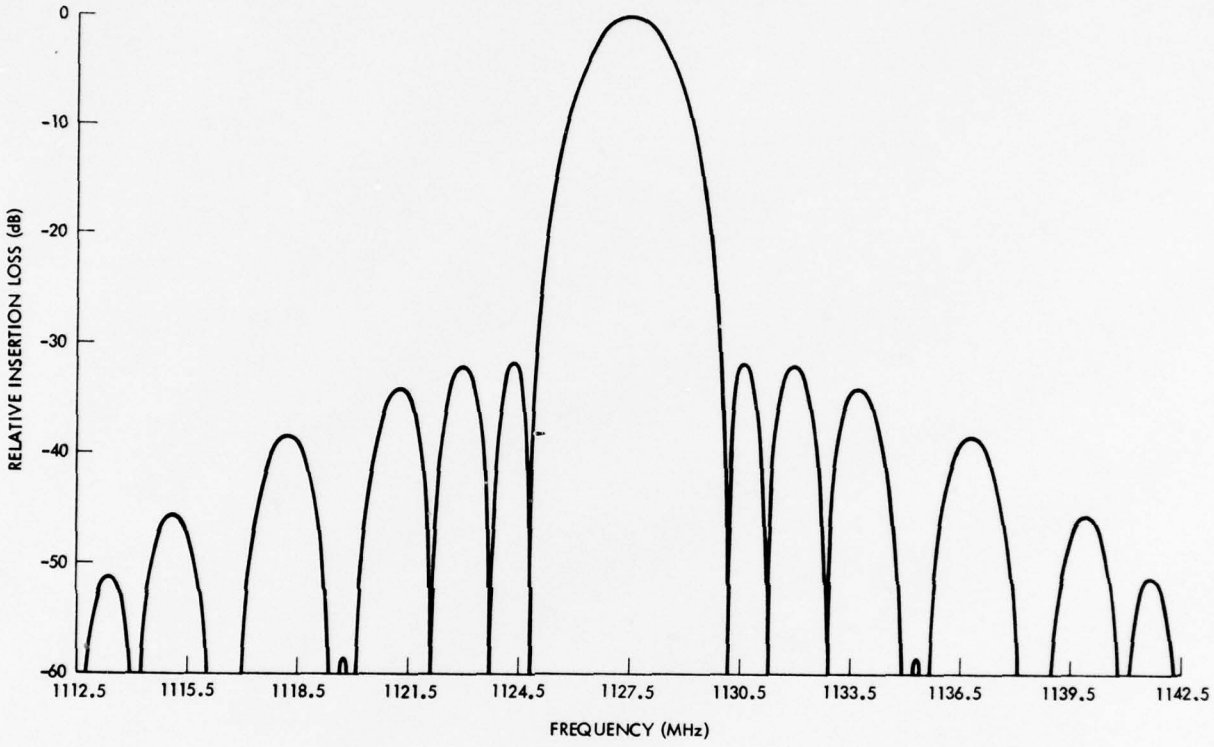

Figure 2-4. Resultant Frequency Response

The equivalent circuit approach was used to calculate the impedance characteristic and the minimum insertion loss of the transducers in the passband. The "cross-field" equivalent circuit model was used since there were many fingers in the transducers. The equivalent circuit of the input admittance of the interdigital transducer is represented by a radiation conductance in parallel with the transducer radiation susceptance and static capacitance. This circuit is illustrated in Figure 2-5.

The radiation conductance is given as

$$G_a(f) = G_o \left(\frac{\sin x}{x}\right)^2 \left(\frac{\sin \hat{N}\pi f_o \tau_o}{\sin \pi f_o \tau_o}\right)^2 \qquad (2.2)$$

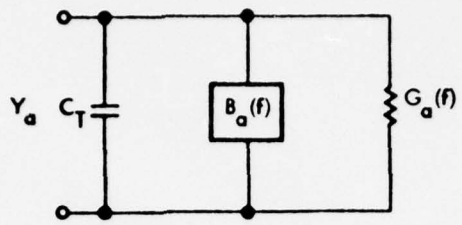

SHUNT "CROSS FIELD" MODEL

Figure 2-5. Shunt Representation for Electrical Input Admittance

where

$G_o = 8\, k^2 N^2 \hat{N} C_T f_o$

k^2 = the piezoelectric coupling constant of the substrate

$C_T = N\, \hat{N}\, C_s\, W_o$

C_s = capacitance per finger pairs

W_o = the aperture of the transducer

Since the transducer is a casual system, the radiation susceptance is given by the Hilbert transform of the radiation conductance

$$B_a(\omega) = \frac{1}{\omega} \int_{-\infty}^{\infty} \frac{G_a(\omega)}{\omega' - \omega}\, d\omega'$$

At the transducer synchronous frequency ω_o

$$B_a(\omega_o) = 0$$

Thus, utilizing the "cross-field" equivalent circuit model, the input admittance or impedance of the transducer (or delay line) can be easily calculated.

Table 2-1 gives a summary of the calculated admittance for the 1 GHz SAW delay line as calculated at the center frequency f_o. The number of finger pairs and the number of sections in both transducers were made identical for photomask fabrication purposes. This results in identical input and output impedances. The total calculated unmatched insertion loss of 25 dB is the sum of the conversion and conduction losses of the transducers plus the propagation loss.

Table 2-1. 1 GHz ST-Cut Quartz SAW Delay Line Calculated Parameters

	Transducer A	Transducer B
Number of sections	30	30
Number of finger pairs per section	4	4
Number of dummy electrodes per section	8	8
Section separations (λ_o)	10	14
Static capacitance (C_T)	3.1 pF	3.1 pF
Transducer input impedance (Z)	9.7 - j43.39	9.7 - j43.39
Transducer conversion loss	≃ 8 dB	≃ 8 dB
Transducer conduction loss	≃ 2 dB	≃ 2 dB
Transducer finger width =	0.7 μm	
Center frequency f_o =	1127.5 MHz	
SAW oscillator Q $\omega_o t$ =	2640	
Propagation loss ≃	5 dB	
Total unmatched insertion loss ≃	25 dB	

2.1.3 1 GHz SAW Delay Line Fabrication

Several special procedures were employed in the fabrication of the 1 GHz delay line. These steps were necessitated by the sub-micron (0.7 μm) transducer finger widths. The basic steps involved in fabricating the delay line are as follows:

- Original photomask generation
- Flexible photomask generation
- Photolithographic processing
- Transducer metallization.

These procedures are described in detail in the following sections.

Photomask Generation

The photomask used in fabricating the 1 GHz SAW delay line was produced for TRW by Electromask. Certain steps were followed to achieve the extremely high tolerances required for the 1 GHz delay line. The 1 GHz SAW delay line used a thin electrode configuration for both the input and output transducers. From Table 2-1, one sees that the number of fingers and sections were identical on each transducer. Only the separation between sections is different. Identical sections were used to minimize the possibility that the two transducers would resonate at two different center frequencies. Only one master section mask was used to generate both the input and output transducers.

The master section of the thin electrode transducer was digitized at 50X the actual size on an Applicon system. The magnetic tape generated by the Applicon system was used to drive a Model 2000 Electromask pattern generator. The pattern generator first flashed the reticle on an anti-reflecting chrome blank at 50X the actual size. Careful measurements were made on the 50X reticle to insure that the transducer section had the required tolerances. After passing acceptance, this reticle was reduced to 10X the actual size on the pattern generator. The final photomask was produced by using the 10X reticle on an Electromask step-and-repeat or image repeater system. This Electromask image repeater used the 10X reticle as the object, flashing it and stopping it while simultaneously reducing it to produce the final photomaster plate.

Conformable Flexible Photomask

The original mask for the 1 GHz SAW delay line was fabricated on a standard 60 mil thick glass plate coated with anti-reflecting chrome. Since the linewidth of the 1 GHz SAW delay line is less than 1 μm wide, it is necessary to transfer this pattern onto a flexible photomask. The use of a flexible photomask minimizes diffraction effects during the ultraviolet exposure of the photoresist on the quartz SAW substrate and insures the linewidth resolution necessary for the submicron linewidth.

Several techniques for transfering the 1 GHz photomask onto the 7 mil thick Corning flexible mask were evaluated. The initial techniques using various types of chemical etching and plasma etching met with limited success. The transducer patterns were successfully transferred several times onto the photoresist, but the final etching step was not successful. The chemical etching resulted in a small amount of undercutting which could not be tolerated for 0.7 μm linewidth. The plasma etching left a residual film which made the results unsatisfactory. The solution was a combination of the two etching processes, that is, plasma etching the chrome down to its last 100 Å and chemically etching the last 100 Å to get the final flexible photomask.

Photolithographic Processing

The flexible photomask was used in conjunction with a vacuum photomask holder to UV expose the photoresist. The submicron linewidths required the use of the lift-off technique. In this process, a dark field flexible mask was used to expose the Shipley 1350J photoresist which was coated onto the quartz substrates. After developing the exposed photoresist, metal is evaporated onto the relief pattern. This technique is schematically represented in Figure 2-6.

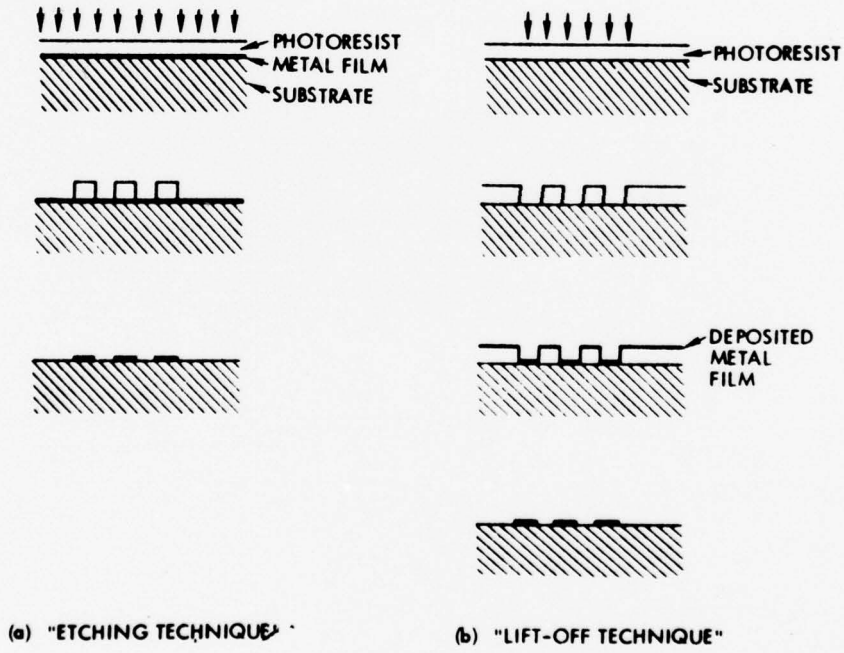

Figure 2-6. Schematic Illustration of Planar Fabrication Technique

In order to achieve maximum linewidth resolution, a conformal vacuum frame using a thin rubber membrane to lift the quartz substrate into intimate contact with the flexible photomask was used. A conformal vacuum frame holder was built using the guidelines developed at MIT Lincoln Laboratory.[1] Figure 2-7 shows the various parts of the conformable vacuum frame holder, and Figure 2-8 shows it assembled and in operation. For the UV exposure, the following sequence of steps is followed. First, the crystal or substrate is held down during alignment by evacuating port 1. The flexible photomask is pulled into intimate contact with the crystal by evacuating port 2. However, the flexible photomask is bowed as it makes intimate contact. In order to eliminate this bowing, the vacuum in port 1 is released to atmospheric pressure. In doing so, the rubber membrane lifts the crystal upward, maintaining intimate contact while eliminating the bowing. The holder is then exposed to UV light which is highly collimated and of uniform exposure illumination.

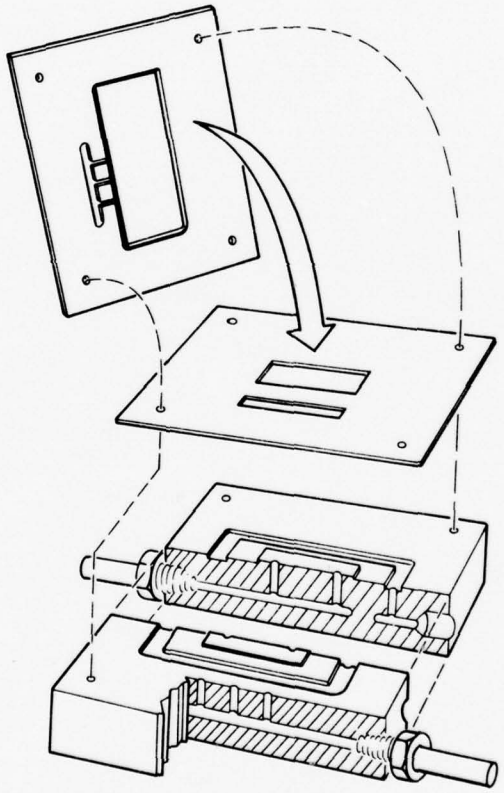

Figure 2-7. Conformable Vacuum Frame

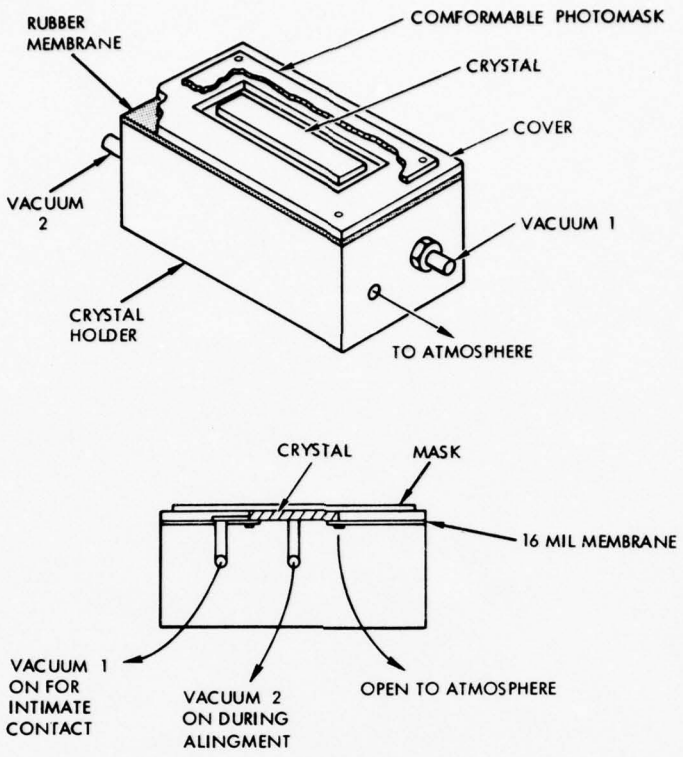

Figure 2-8. Vacuum Frame Operational Details

Transducer Metallization

The metallization film thickness has a great effect on the performance of the SAW delay line. The metal film thickness is determined as a result of a compromise between the requirements for a thin film to minimize second order effects and a thick film to minimize resistive losses. This problem was solved by employing different film thicknesses for the transducers and sum bars.

The delay line was fabricated using the lift-off technique. The quartz substrate was first cleaned and coated with Shipley 13500 photoresist. The relief pattern was formed using a conformal mask. However, instead of the usual chromium and aluminum film metallization thicknesses, only 300 Å of aluminum was evaporated onto the substrate. After removal of the unwanted metallization to expose the transducer patterns, the delay line was recoated with photoresist and exposed with a second mask which allowed additional metallization of just the sum bars and bond pads. After developing this pattern, an additional 1000 Å of aluminum was evaporated into the relief pattern. This added metallization insured good ultrasonic wire bonds and low resistive loss in the sum bars.

2.2 TEMPERATURE-COMPENSATED SAW DELAY LINE FABRICATION

Temperature-compensated SAW delay lines can be fabricated using composite structure substrates. The compensated substrate evaluated by this program consisted of a thin film of silicon dioxide (SiO_2) sputtered onto a YZ cut lithium tantalate ($LiTaO_3$) crystal. These two materials each have linear first order temperature coefficients, but they are of opposite sign. $LiTaO_3$ has a negative temperature coefficient of -35×10^{-6} per °C which is determined by the bulk properties of the crystal. The SiO_2 film has a positive temperature coefficient. The acoustic wave propagates through both the SiO_2 film and the $LiTaO_3$ substrate. By controlling the SiO_2 film thickness, hence the relative density of the acoustic wave in the two materials, the two opposite temperature coefficients of delay can be made to cancel. The distribution of the acoustic wave energy between the two materials is determined by the thickness of the SiO_2 film (t) expressed as a fraction of the acoustic wavelength (t/λ). Therefore, for the proper t/λ ratio, a delay line with a net first order temperature coefficient can be fabricated. This section describes the fabrication of the composite structure delay lines, the testing of these delay lines is covered in Section 4.2.

The $SiO_2/LiTaO_3$ composite delay lines were fabricated by RF sputter depositing SiO_2 onto a $LiTaO_3$ substrate. The interdigital transducers were fabricated onto the $LiTaO_3$ substrate prior to sputtering the SiO_2. This sequence is required because SiO_2 is non-piezoelectric and therefore, the transducers must be fabricated onto the $LiTaO_3$. Figure 2-9 shows the configuration of a typical composite structure delay line. The sum bars are extended behind the transducers and this area is masked from the SiO_2 deposition to allow wirebonding to the sum bars.

Several $SiO_2/LiTaO_3$ composite structure SAW delay lines were fabricated. These delay lines operated at center frequencies of approximately 650 MHz. The delay line photomask, originally designed for ST-cut quartz, used thin electrode transducers. Due to the 1.33 µm finger dimension of these delay lines, the lift-off technique as described in Section 2.3 was employed in their fabrication.

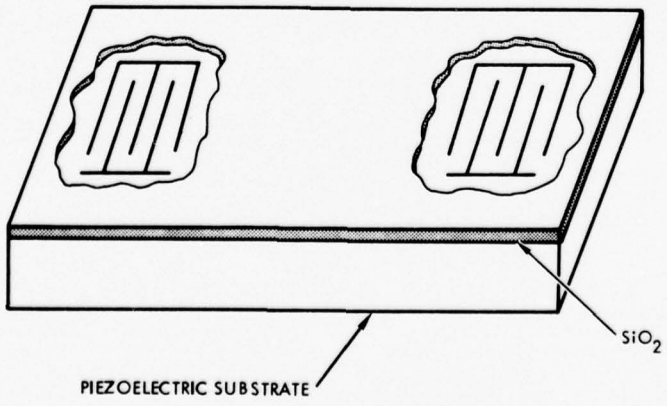

Figure 2-9. Configuration of $SiO_2/YZ\text{-}LiTaO_3$ Composite Structure

An R. D. Mathis sputtering system was used to RF-sputter deposit the SiO_2 onto the $LiTaO_3$ SAW delay lines. Several parameters of the sputtering environment were varied in order to obtain the optimum performance. The compensated structures were all sputtered continuously in a pure oxygen environment. Previous theoretical and experimental* work has indicated a SiO_2 t/λ ratio of 0.573 is required for temperature compensation. This result was obtained for an oscillator operating at approximately 340 MHz. Based on these results, a SiO_2 film thickness of 3.04 μm would be required.

The first composite structure delay line had a 1.27 μm SiO_2 film ($T/\lambda = 0.24$) which was deposited continuously for 33 hours at a rate of 0.0384 μm/hour. The SiO_2 film was of uniform thickness and exhibited no defects. This delay line had approximately one half the required SiO_2 thickness required for complete temperature compensated and was fabricated to obtain an intermediate data point between no compensation and complete temperature compensation. The measured coefficient for this delay line was -14.3×10^{-6} per ^{o}C. Based on a linear interpolation of the previous measurements, the predicted coefficient for this delay line is -14.7×10^{-6} per °C. However, theoretical calculations do not predict a simple linear dependence.[1] Thus, the measured value of -14.3 ppm/^{o}C is in reasonable good agreement.

Prior to fabricating the second composite structure delay line, the sputtering system was modified to increase the deposition rate to 0.21 μm/hour. The second temperature compensated delay line was sputtered at this rate for 13.1 hours which yielded an SiO_2 film thickness of 2.75 μm ($t/\lambda = 0.52$). Even at this higher deposition rate, the SiO_2 film exhibited no defects and was of uniform thickness. The temperature coefficient of this delay line was $+3.5 \times 10^{-6}$ per °C, which indicates that the SiO_2 film thickness was slightly greater than required for complete compensation.

The measured temperature coefficients as a function of t/λ for these two delay lines are plotted in Figure 2-10, previous data for an uncompensated $LiTaO_3$ crystal is also shown for reference. The data has been interpolated to determine the required t/λ to achieve a zero first order coefficient. The required ratio is 0.491 which would be achievable with a final iteration.

---

*T.E. Parker and H. Wichansky, "Material Parameters of the Temperature-Stable SiO_2.TZ $LiTaO_3$ Structures," IEEE 1975 Ultrasonic Symposium, September 1975, pp. 503-507.

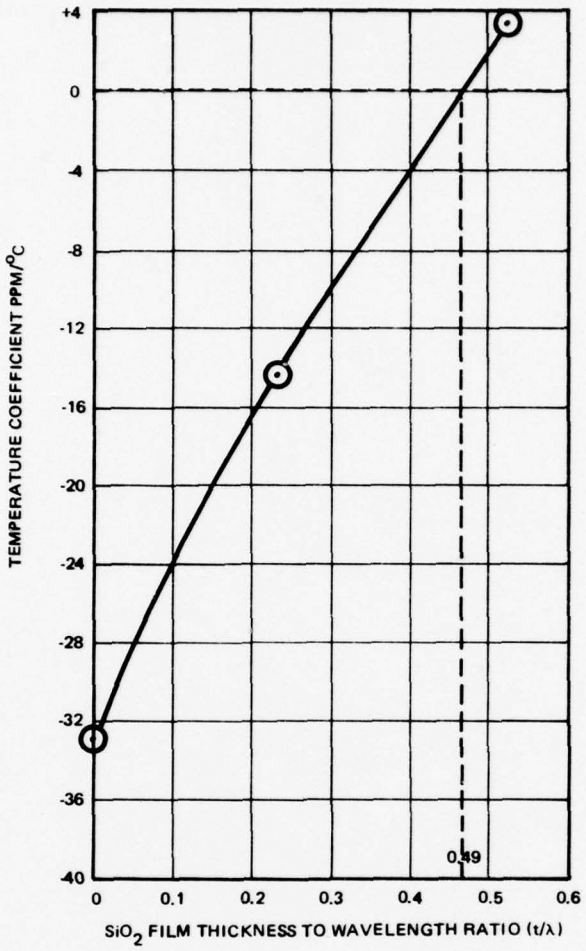

Figure 2-10. $SiO_2/LiTaO_3$ Composite Structure Temperature Coefficient

3. SAW OSCILLATOR DESIGN AND FABRICATION

This section discusses the theory of operation of SAW oscillators and then describes the way in which this theory was implemented in the fabrication of the SAW oscillators for this program.

3.1 THEORY OF OPERATION OF SAW OSCILLATOR

A SAW oscillator consists of a SAW delay line connected in a feedback loop with an amplifier. This is shown schematically in Figure 3-1. This circuit will oscillate at any frequency for which the total phase shift around the loop is an integer multiple of 2π, and the gain of the amplifier is equal to or greater than the net insertion loss of the feedback elements. The conditions for oscillation can be expressed as:

$$\frac{2\pi f \ell}{V} + \phi = 2n\pi \tag{3.1}$$

and

$$L_S(f) + L_1(f) = G(f, A) \tag{3.2}$$

where

f = oscillation frequency

ℓ = center to center transducer separation

V = surface wave velocity

ϕ = phase shift through all elements except SAW delay line

n = an integer

$L_S(f)$ = insertion loss of SAW delay line

$G(f, A)$ = amplifier gain as a function of f and output level, A

Solving (3.1) for f

$$f = \frac{V}{\ell}\left(N - \frac{\phi}{2\pi}\right) \tag{3.3}$$

As a general rule, $L_1(f)$ and $G(f,A)$ are very slowly varying functions of f over a broad range around the frequency for which the oscillator is being designed, but $L_S(f)$ is a very strong function of frequency. The SAW delay is designed as a bandpass filter whose response is ideally given by

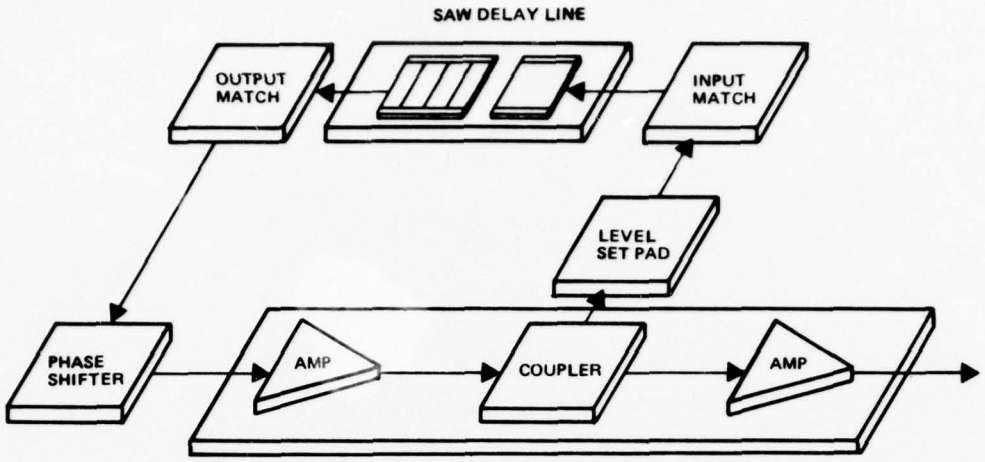

Figure 3-1. Schematic of SAW Oscillator

$$L_S(f) = K \left(\frac{\sin X}{X}\right)^2 \left(\frac{\sin Y}{Y}\right)^2 \tag{3.4}$$

where

$$X = \frac{2\pi N(f-f_o)}{f_o}$$

$$Y = \frac{2\pi M(f-f_o)}{f_o}$$

K = insertion loss at f_o

N = number of finger pairs in first transducer

M = number of finger pairs in second transducer

$$K \left[\frac{\sin\left(\frac{2\pi N(f-f_o)}{f_o}\right)}{\frac{2\pi N(f-f_o)}{f_o}}\right]^2 \left[\frac{\sin\left(\frac{2\pi M(f-f_o)}{f_o}\right)}{\frac{2\pi M(f-f_o)}{f_o}}\right]^2 = G(f_o, A) - L_1(f_o) \tag{3.5}$$

It is clear that proper oscillator operation will occur when (3.3) is satisfied only for f_o. Equation (3.3) has nearly n solutions, but the gain term of (3.5) can be adjusted such that the only simultaneous solutions to both (3.3) and (3.5) occur at f_o. The fact that the appropriate adjustment of the gain term is possible is evident

from Figure 4-3 which clearly shows a minimum of 8 dB difference between the response at f_o and any secondary responses. So long as only one solution to (3.3) falls within the primary response of the SAW delay line, single mode operation of the SAW oscillator is guaranteed.

It is also evident from (3.3) that some frequency modulation of the SAW oscillator is possible. Taking the derivative

$$\frac{dF}{f} = \frac{-Vd\phi}{2\pi\ell\phi}$$

This gives the expected result that the smaller the center to center transducer separation, i.e., the lower the delay line Q, the greater the SAW oscillator tuning range. The usual method of accomplishing the tuning or frequency modulation is via a varactor diode phase shift network.

3.2 SAW OSCILLATOR FABRICATION

In addition to the SAW delay line, a feedback amplifier and a power splitter are required to complete the SAW oscillator circuit. A selectable phase shifter and an attenuator are also included in the circuit to aid in evaluating and optimizing the oscillator performance.

A single, common amplifier was selected for use in all of the SAW oscillators. The amplifier, manufactured by Aertech Industries, is a multistage thin film MIC transistor design. The amplifier was specifically designed for use as the loop amplifier in SAW oscillators. The broad bandwidth (200 to 1100 MHz, high gain (>30 dB), low noise figure (<5 dB), and high reverse isolation (>15 dB) were specified for optimum flexibility and performance in SAW oscillators. The amplifier was designed to have an internal power divider and an output buffer stage, as shown schematically in Figure 3-1. The purpose of the amplifier stage following the power splitter is to provide active isolation between the oscillator loop and the oscillator head. Table 3-1 summarizes the typical performance parameters for the loop amplifiers. The reamining electronic components required for the oscillator are a phase shifter and a level set attenuator. The phase shifter is used to fine tune the frequency of the oscillator. For this application, maximum phase shift with minimum amplitude variation is required. The 1 dB bandwidth of the phase shifter is $\simeq \pm 45^{o}$. The schematic for the phase shifter is shown in Figure 3-2. It was assembled using a hand wound transformer for the 90^{o} hybrid and variable capacitors.

The attenuator in the feedback loop was simply a "tee" configuration attenuator utilizing composition resistors. The values of the resistors were selected to provide the required level of attenuation. The value of attenuation is determined by the difference between the delay line insertion loss and the linear amplifier gain. The

Table 3-1. Feedback Amplifier Specification

Frequency range	100 to 1600 MHz
Gain	30 dB min
Power out	7 dBm min
Noise figure	5 dB max
VSWR	2.0:1 max
Isolation	15 dB min
Gain variation over temp	± 1 dB max
Power consumption	100 mA @ 15 V max

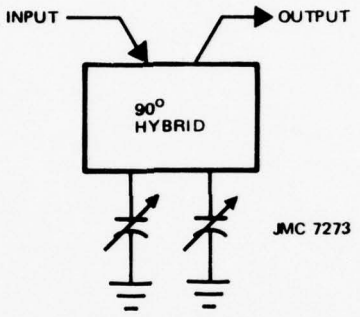

Figure 3-2. Fine Tuning Phase Shifter for SAW Oscillator

attenuator in the loop is then changed so that there is approximately 3 dB of excess gain in the loop. The amount of excess linear amplifier gain determines the level of saturation in the amplifier when the loop is oscillating. Regardless of the amount of excess linear loop gain, when the loop is oscillating, the amplifier will saturate or compress until the total gain around the loop is reduced to unity.

The 3 dB of excess loop gain is a compromise between several factors. A higher level of excess gain in the loop would result in greater output power from the oscillator and would provide a greater assurance that the loop will continue to oscillate if the delay line insertion loss increases or the amplifier gain decreases due to the effects of aging and temperature. However, high levels of excess loop gain and therefore saturation result in an increase in the amplifier noise figure (or oscillator phase noise) and in higher levels of harmonically related spurious outputs.

With the exception of the delay line which is mounted in a hermetically sealable flatpack, all of the loop electronics are assembled onto a single 1.7 x 2.0 inch alumina microstrip substrate. The loop amplifier is contained in a hermetic 22 pin package. The package is mounted on the ground plane side of the substrate using conductive epoxy. The loop attenuator, phase shifter, bias de-coupling network, and interconnecting circuitry are all on the top side of the substrate. The substrate

is soldered to a kovar frame which is attached to the oscillator housing with screws. A spring finger frame under the substrate insures a good ground contact between the substrate ground plane and the housing. Prior to mounting the SAW delay line into the package, the package is soldered to a carrier plate. This plate is then firmly attached to the oscillator housing. This technique insures a good ground path between the delay line and loop electronics which is important for stable oscillator performance as a function of temperature. If there is an intermittent or unstable ground, the oscillator will skip in frequency as the oscillator is temperature cycled. The completed SAW oscillators were assembled into a machined 3.25 x 2.5 x 0.7 inch housing which weighs less than 0.2 pound.

4. SAW OSCILLATOR DEVELOPMENT

4.1 1 GHz SAW OSCILLATOR

The fabrication and test of the 1 GHz SAW oscillator was a multistep process. The five separate tasks involved were as follows:

- 1 GHz SAW delay line design and fabrication
- SAW oscillator loop electronics fabrication and test
- SAW delay line packaging and characterization
- SAW oscillator overall integration and alignment
- SAW oscillator characterization.

The first two tasks were described in Sections 2 and 3. The remaining tasks are described in this section. A photograph of the complete 1 GHz oscillator is shown in Figure 4-1.

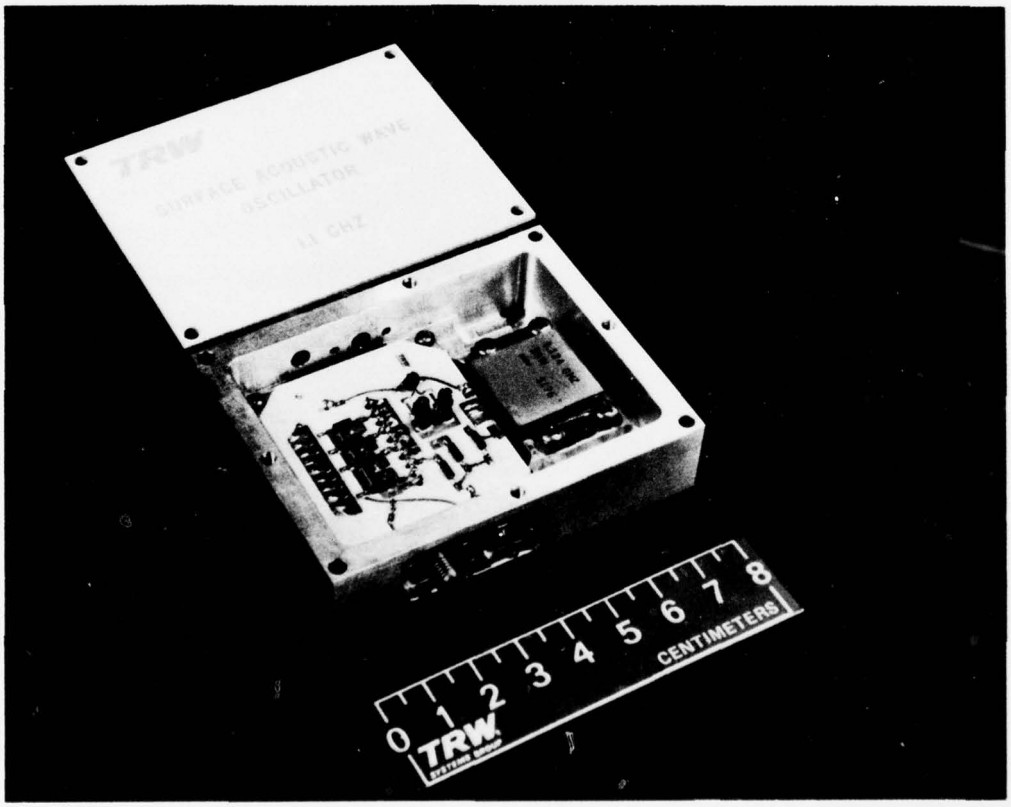

Figure 4-1. 1 GHz SAW Oscillator

4.1.1 SAW Delay Line Packaging and Characterization

After fabrication, the SAW delay line was mounted in a microelectronic flatpack for use in assembling the SAW oscillator. The SAW delay line was hermetrically sealed for two reasons: first to mechanically protect the SAW crystal and, second, to provide a noncontaiminating environment for the SAW device. The first includes environmental considerations such as protecting the crystal from damage and stabilizing the crystal with respect to shock and vibration. The second set of requirements is more subtle and relates to minimizing the long-term aging rate of the complete SAW oscillator. The total delay through the SAW delay line (and hence the SAW oscillator frequency) is very sensitive to any contamination on the surface of the SAW crystal. For this reason the delay line must be cleaned and hermetically sealed.

A photograph of the packaged 1 GHz SAW delay line mounted in the flatpack is shown in Figure 4-2. Prior to installing the SAW crystal, the flatpack was soldered to a carrier plate and a ground shield was added inside the package. The crystal was then mounted in the package using an RTV material as the adhesive. Input, output, and ground connections to the flatpack terminals were made with aluminum bond wires.

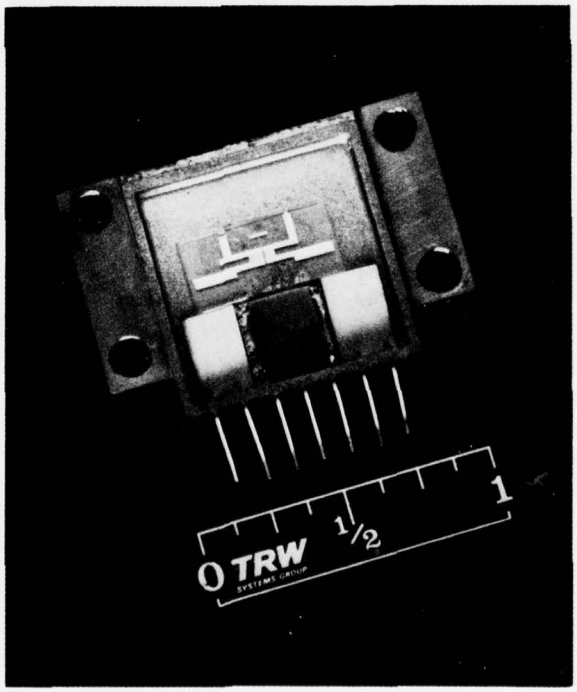

Figure 4-2. 1 GHz SAW Delay Line

Prior to sealing, the delay line was characterized. Figure 4-3 shows the results of these tests. The delay line insertion loss was measured for both the unmatched condition and after the device input and output were matched, using triple stub tuners. The measured unmatched insertion loss was 32 dB, which was reduced by matching to 26 dB. Finally, the delay line was sealed and the passband characteristics were re-checked.

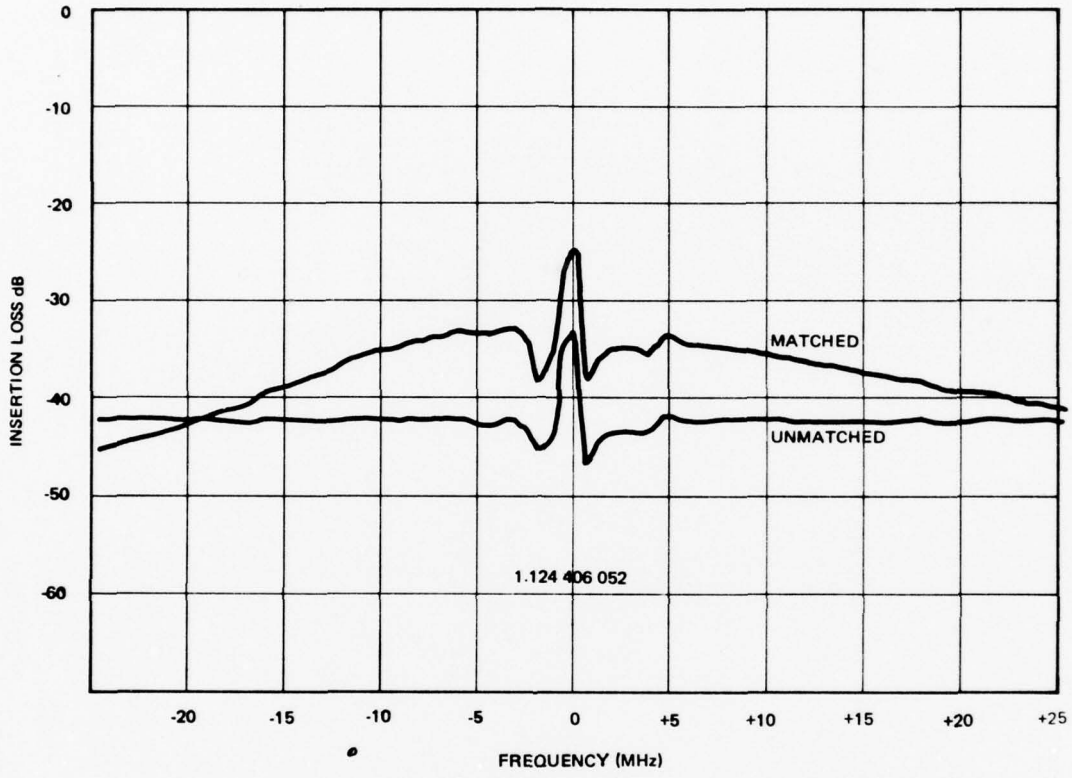

Figure 4-3. Delay Line Test Results

4.1.2 1 GHz SAW Oscillator Alginment

The alignment process for the oscillator is relatively uncomplicated. The primary requirement in aligning the oscillator is to set the residual phase shift (all phase shift not in the SAW delay line) around the loop so that the net phase shift is $2n\pi$ at the desired frequency of operation. Provisions were made for both coarse and fine tuning the loop phase shift. Coarse tuning is accomplished using a coaxial delay cable phase shifter to set the oscillator to the exact desired frequency of operation. Fine tuning is accomplished using a variable capacitor (described in Section 3.2). The oscillator can be fine tuned over a ±100 ppm range with a tuning resolution of ±1.

4.1.3 SAW Oscillator Characterization

The characterization testing of the 1 GHz SAW oscillator included temperature stability, phase noise, and sensitivity to load VSWR and input voltage variations. The results of these tests are summarized in Table 4-1.

Table 4-1. 1 GHz SAW Oscillator Characterization Summary

Parameter	Performance
Output frequency	1.124 GHz
Output power	+12.0 dBm
Temperature stability	
-40°C to +80°C	
Frequency	±180 ppm
Power	±0.4 dB
Phase noise	-82 dBc/Hz at 1 kHz
	-150 dBc/Hz at 1 MHz
Load VSWR sensitivity	
1.7:1 All phases	
Frequency	±10 ppm
Power	±1 dB
Input voltage sensitivity (±5%)	
Frequency	±3 ppm
Power	±0.5 dB
DC power (+15 V)	1.15 watt
Size	3.25 x 2.55 x 0.75 inches
Weight	0.38 lb

The temperature dependence (medium term stability) of the 1 GHz SAW oscillator was measured over the range of -40 to +80°C. The measured data is shown in Figure 4-4. The shape of the oscillator frequency vs. temperature curve is determined by the temperature coefficient of the ST-cut quartz SAW delay line. This material theoretically has a zero-first order temperature coefficient of delay near room temperature and a second order coefficient of $-31 \times 10^{-9}/°C^2$. This response has

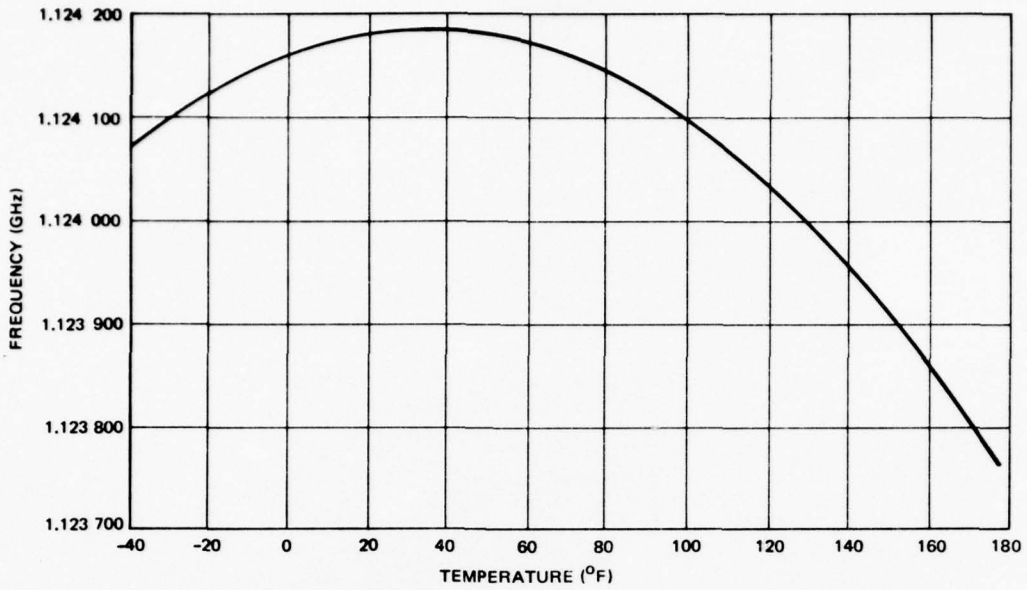

Figure 4-4. Temperature Effects on Oscillator Frequency

been previously verified for low frequency SAW devices (250 MHz), but has been shown not to hold true at higher frequencies. At higher frequencies, the temperature at which the minima occurs shifts downward in temperature, but the second order coefficient does not change. This shift in temperature for high frequency oscillators is currently not completely explained, but it is felt to be due to second order effects created by the transducer metallization. The measurements of the 1 GHz oscillator confirm the previous data. Although the minima has shifted to +40°F, the second order coefficient of the response is $-30.6 \times 10^{-9}/°C^2$, which compares favorably with the predicted value of $-31 \times 10^{-9}/°C^2$. The frequency variation over the -40°F to +110°F range was $\pm$50 ppm and the variation was $\pm$180 ppm over the full -40°F to +175°F range.

Figure 4-5 shows the output power versus temperature for the oscillator. The power variation is mainly dependent on the saturated output power variation of the loop amplifier. The output power variation was less than 0.8 dB over the full -40°F to +175°F range and was less than 0.5 dB over the 0°F to +100°F range. With simple temperature compensation in the amplifier bias circuitry and by optimizing the amplifier saturation characteristics, it should be possible to reduce the variation to less than 0.5 dB over the full -50°F to +150°F temperature range.

The frequency domain phase noise of the oscillator was measured using a single oscillator technique, utilizing a coaxial delay line FM discriminator. This technique enables noise measurements to be made very close to the carrier with a high level of accuracy. A triple stub tuner, phase shifter, and coaxial delay line

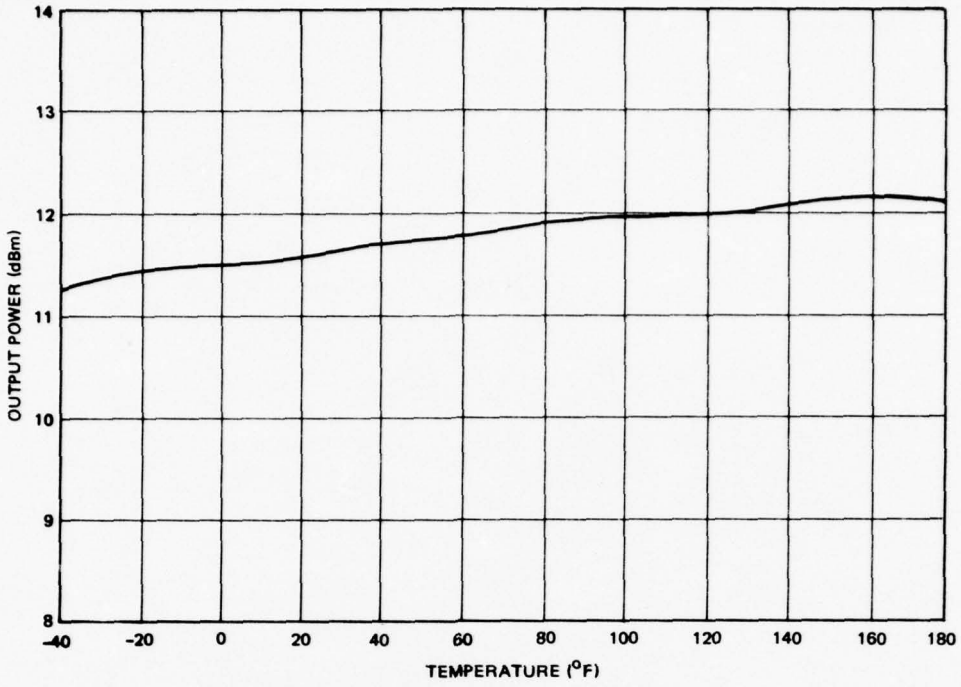

Figure 4-5. 1 GHz SAW Oscillator Output Power vs Temperature

cable comprise an FM discriminator. The reference and signal inputs to the double balanced mixer are in phase quadrature to make an accurate measurement close to the carrier. The detected output of the mixer is passed through a 15 MHz low pass filter and into the tracking spectrum analyzer which is controlled by the automatic frequency synthesizer. The phase noise measurements were made for offset frequencies of 10 Hz to 1 MHz.

The measured phase noise for the oscillator is given in Figure 4-6. As expected, the noise decreases at a 20 dB per decade $(\frac{1}{f^2})$ rate. The results are not accurate for offset frequencies greater than 1 MHz due to resonances in the coaxial delay line which produce peaks and nulls in the phase noise plot above 1 MHz.

The final tests performed on the 1 GHz SAW oscillator were to determine the effects of load VSWR and supply voltage variations on output power and frequency. The load VSWR sensitivity of the oscillator was measured using a known return loss load and a line stretcher. In this fashion, the worst case variation for all phase angles was determined. Figure 4-7 is a plot of the results. The oscillator pulling is less than $\pm$10 ppm for all phase angles of a 1.7:1 load VSWR. The last test was to determine the oscillator sensitivity to input voltage. For a $\pm$5% input voltage variation, the frequency variation was $\pm$3 ppm and the power variation was $\pm$0.5 dB.

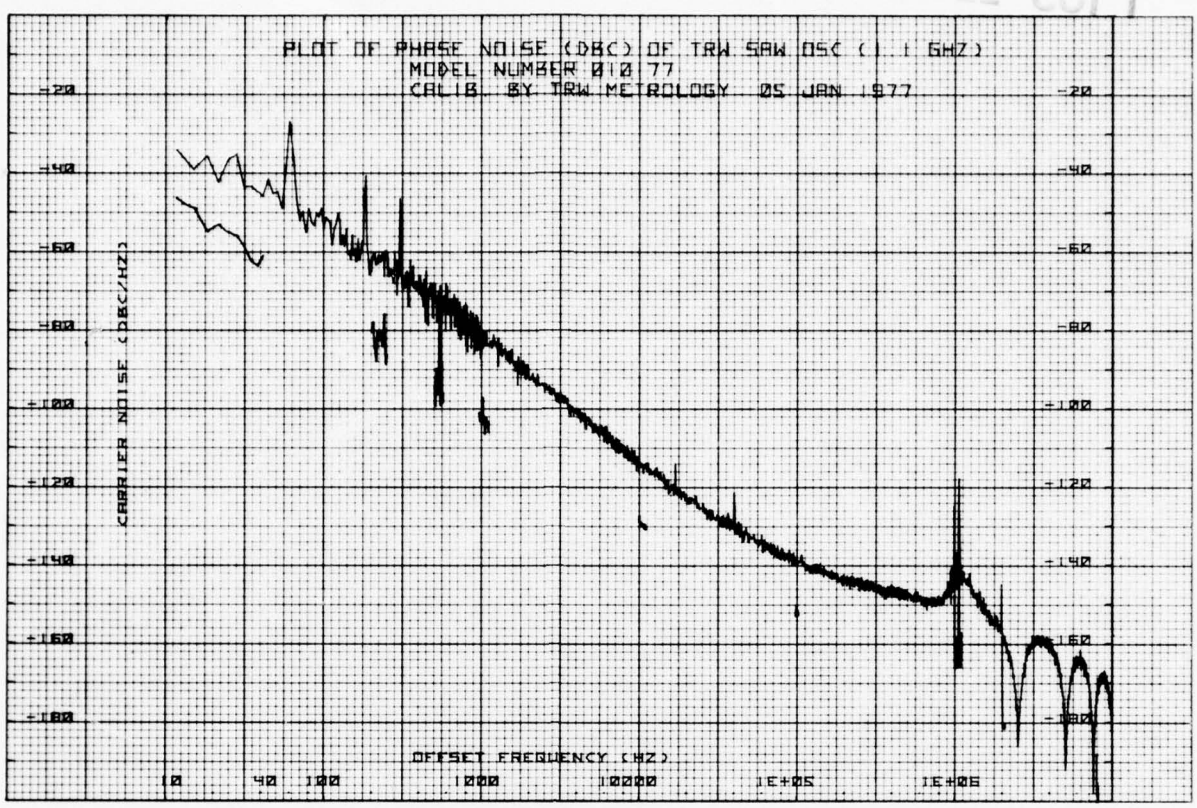

Figure 4-6. 1.124 GHz SAW Oscillator Phase Noise Measurement

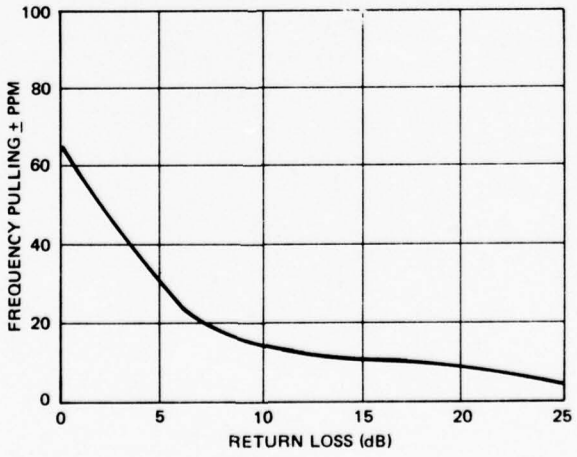

Figure 4-7. 1 GHz Load Pulling Characteristics

4.2 SAW OSCILLATOR TEMPERATURE COMPENSATION

The temperature stability of a SAW oscillator is primarily determined by the temperature coefficient of the SAW delay line. For an uncompensated SAW oscillator, ST-cut quartz has been widely used because of its high inherent temperature stability. ST-cut quartz has a zero first order temperature coefficient of delay near room temperature and a second order coefficient of $+31 \times 10^{-9}/°C^2$. Therefore, the theoretical temperature stability of a SAW oscillator using a ST-cut quartz delay line is $\pm 0.01\%$ over the -40 to +175°F range. In many system applications, this degree of temperature stability is not sufficient and techniques for improving the temperature stability of SAW oscillators are required. Two basic approaches were investigated: temperature compensation of the delay line and temperature compensation of the oscillator electronics

4.2.1 Temperature Compensated SAW Delay Line

The temperature compensated SAW delay line consists of a uniform layer of silicon dioxide (SiO_2) deposited on a YZ lithium tantalate ($LiTaO_3$) substrate. These two materials each have linear first order temperature coefficients, but are of opposite sign. Therefore, with the proper SiO_2 film thickness the two temperature coefficients will cancel and the net coefficient will be zero. A complete discussion of the design and fabrication of the temperature compensated delay line is contained in Section 2.3.

The first step in this investigation was to measure the temperature coefficient of the $LiTaO_3$ substrate. This was accomplished using a 224 MHz SAW delay line and oscillator electronics. The measured coefficient was -35.5×10^{-6} per °C, which closely agrees with the theoretical -35.1×10^{-6} per °C temperature coefficient for $LiTaO_3$.

Two 650 MHz temperature compensated SAW delay lines were then fabricated and tested. The first delay line was coated with 1.27 μm of SiO_2, which is slightly less than the required thickness for complete compensation. The calculated temperature coefficient for this delay line was -14.7×10^{-6} °C. The measured coefficient was -14.3×10^{-6} per °C, which corresponds to a frequency variation of ±0.08% over the -40 to +70°C range. The second compensated delay line had an SiO_2 film thickness of 2.75 μm. The measured temperature coefficient of this delay line was $+3.5 \times 10^{-6}$ per °C. Over the temperature range of -40 to +70°C, the total frequency variation was ±0.035%. The results of the frequency vs temperature tests for all three delay lines are shown in Figure 4-8. The graph illustrates the effect of increasing SiO_2 film thickness on both the magnitude and sign of the oscillator temperature coefficient.

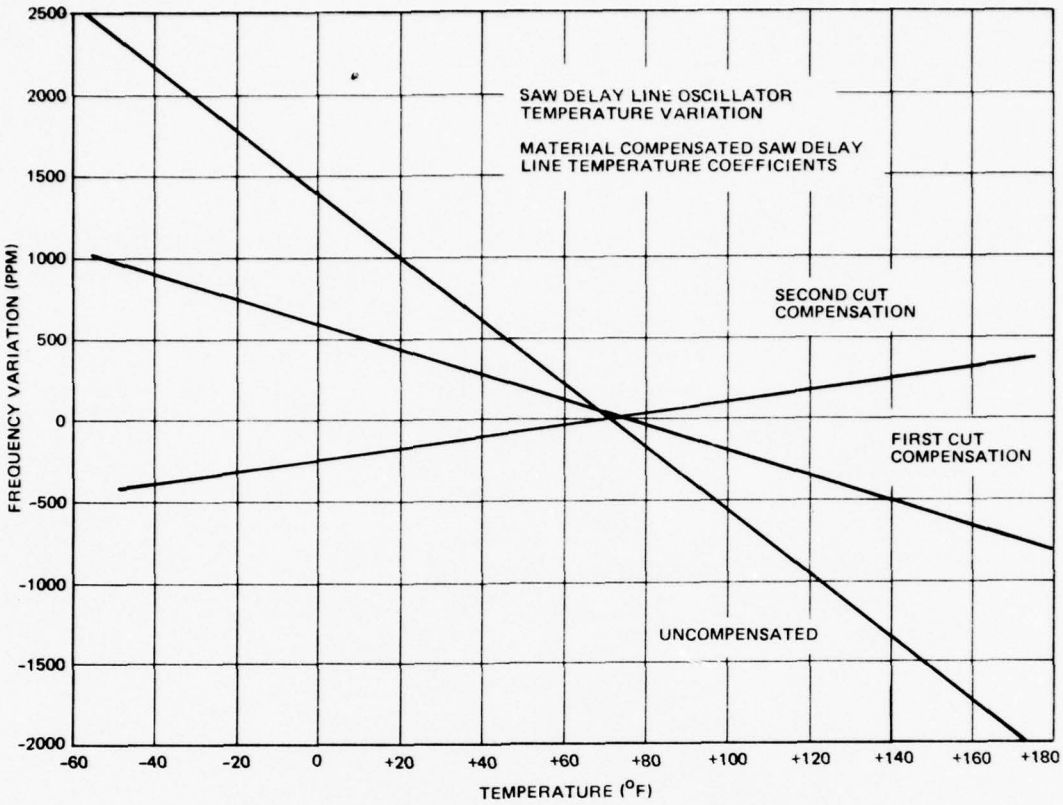

Figure 4-8. Material Components SAW Delay Line Temperature Coefficients

These tests have demonstrated the technique of producing a temperature compensated SAW delay line using a composite substrate structure. Several data points were measured and the sign of the temperature coefficient of the delay line was demonstrated to be a function of the thickness of the SiO_2 film. A temperature stability of $\pm$0.035% was achieved. With an additional iteration of the SiO_2 film thickness, it should be possible to reduce this variation to under $\pm$0.01%, which is comparable to ST-cut quartz.

4.2.2 Electronically Temperature Compensated SAW Oscillator

An electronically temperature compensated SAW oscillator consists of an uncompensated SAW delay line oscillator which is tuned or corrected as a function of temperature by an electronic network so as to maintain a constant output frequency. The oscillator contains two basic circuits: a SAW VCO and a compensation drive circuit for the VCO. The drive circuit may be either analog or digital.

The first task in the development of the temperature compensated oscillator was the design of the SAW VCO. For the 250 MHz SAW oscillator which was being compensated, the frequency variation over the temperature range of -40 to +180°F range was 40 kHz. Therefore, the SAW VCO must have a total electronic tuning

range of greater than 40 kHz. In actual practice, the desirable range would be approximately twice the expected variation so as to provide sufficient design margin.

Referring back to equation (3.6)

$$\frac{d_f}{f} = \frac{-V d\phi}{2\pi \ell \phi} \qquad (3.6)$$

it is evident that the SAW oscillator can be frequency tuned by varying the remaining loop phase shift outside of the SAW delay line. An electronic phase shifter utilizing a 90° hybrid and two varactor diodes was designed for this purpose. The phase range requirement for the phase shifter can be calculated by measuring the phase tuning sensitivity of the oscillator using a calibrated phase shifter in the loop. For the 250 MHz oscillator, the tuning rate was 1.5 kHz per degree of phase shift which translates for the desired frequency range of 80 kHz to a phase shift of approximately 55°. The loop phase shifter circuit is shown in Figure 4-9. The circuit has a 1 dB tuning bandwidth of approximately 75°. Minimal (<1 dB) amplitude variation as a function of tuning voltage is critical to maintaining stable oscillator loop performance.

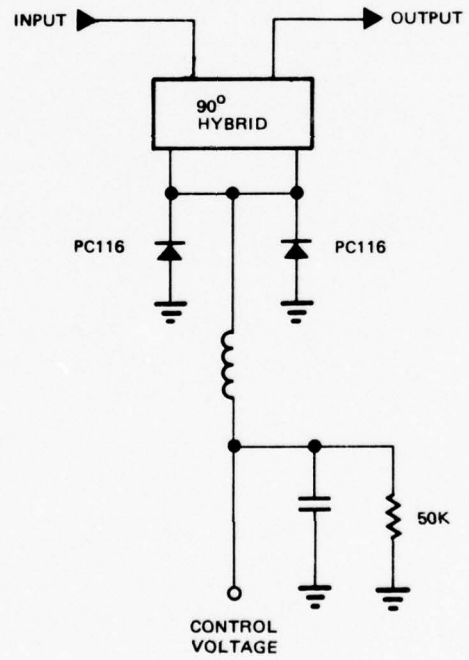

Figure 4-9. Varactor Tuned Phase Shifter

A fixed tuned 250 MHz SAW oscillator design was modified to operate as a SAW VCO. The meander line phase shifter substrate previously used to mechanically fine tune the oscillator frequency was replaced by the electronic phase shifter circuit. The resulting output frequency as a function of control voltage is shown in Figure 4-10. The oscillator had a tuning range of 110 kHz ($\pm$0.02%) for a 0 to +10 volt control voltage swing. In addition, the tuning characteristic was extremely linear. The SAW VCO was next temperature tested to determine the tuning voltage required to maintain a constant frequency as a function of temperature. The measured data is shown in Figure 4-11. As would be expected, based on the knowledge of the temperature characteristic of the SAW delay line, the curve was approximately parabolic.

As stated earlier, the network that generates the control voltage as a function of temperature can be either analog or digital. Analog techniques were evaluated, but were found to be unsatisfactory due to the complex shape of the required voltage vs temperature characteristic. For this reason, a digital technique was used.

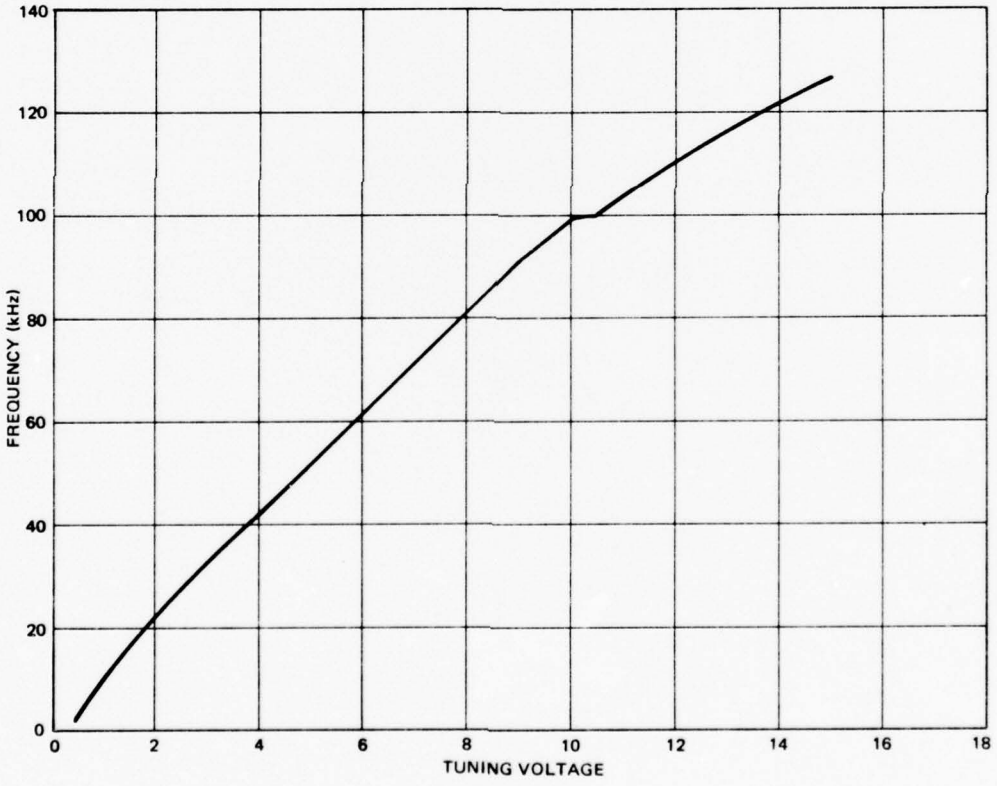

Figure 4-10. SAW VCO Output Frequency Shift as a Function of Tuning Voltage

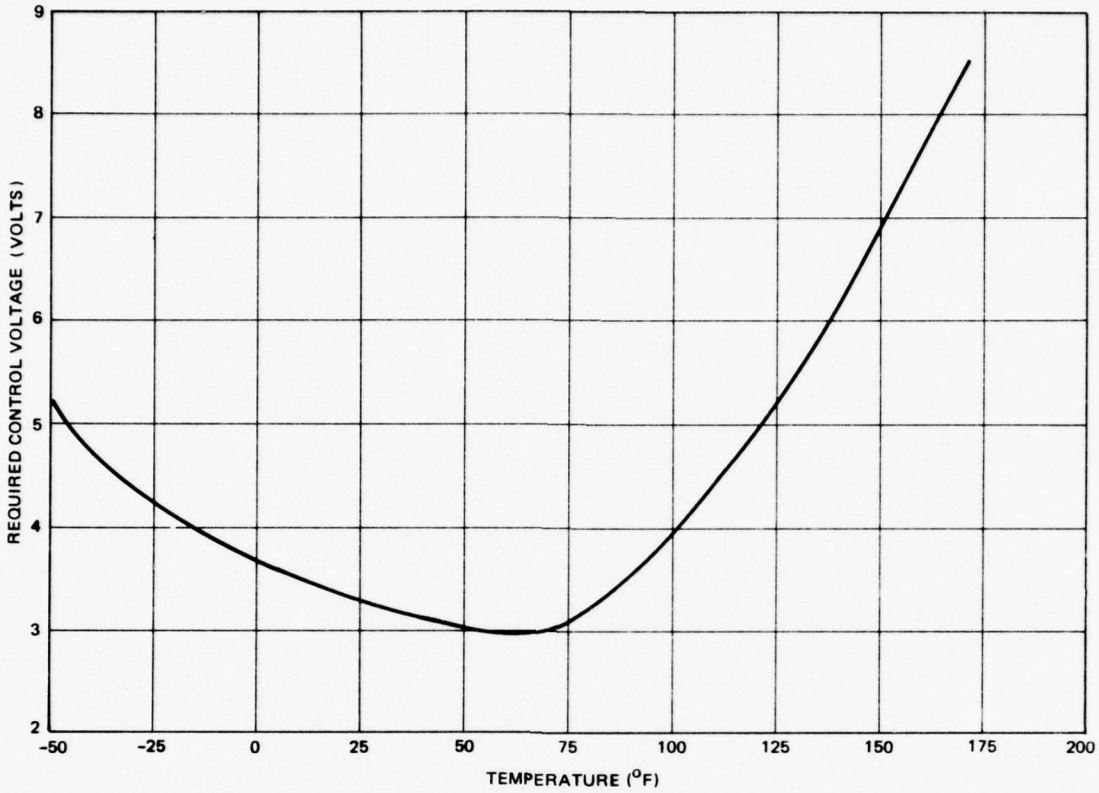

Figure 4-11. Tuning Voltage Required to Stabilize SAW Oscillator as a Function of Temperature

The digital temperature compensation technique proved to be extremely successful. The temperature compensation was achieved by storing in a digital memory a table of correction voltages to be applied to the SAW VCO as a function of temperature. A basic block diagram of the circuit is shown in Figure 4-12. The circuit functions as follows. A sensitor (positive temperature coefficient resistor and a fixed resistor are configured as a voltage divider to provide a reference voltage as a function of temperature. The voltage is then analog-to-digital (A/D) converted into a 6-bit word. The sensitor and resistor values are selected so that the resulting voltage swing as a function of the required temperature range corresponds to the full input dynamic range of the A/D converter. The digital word out of the A/D converter, which indicates the oscillator baseplate temperature, is then used as the input address to a programmable read only memory (PROM). The output of the PROM is then D/A converted. The resulting output current is converted to a tuning voltage for the SAW VCO with an operational amplifier. The op-amp gain is set so that the full dynamic range of the D/A output corresponds to the desired VCO tuning voltage range. The oscillator is then aligned by measuring the output of the A/D converter as a function of temperature and the input word to the D/A converter required to return the oscillator

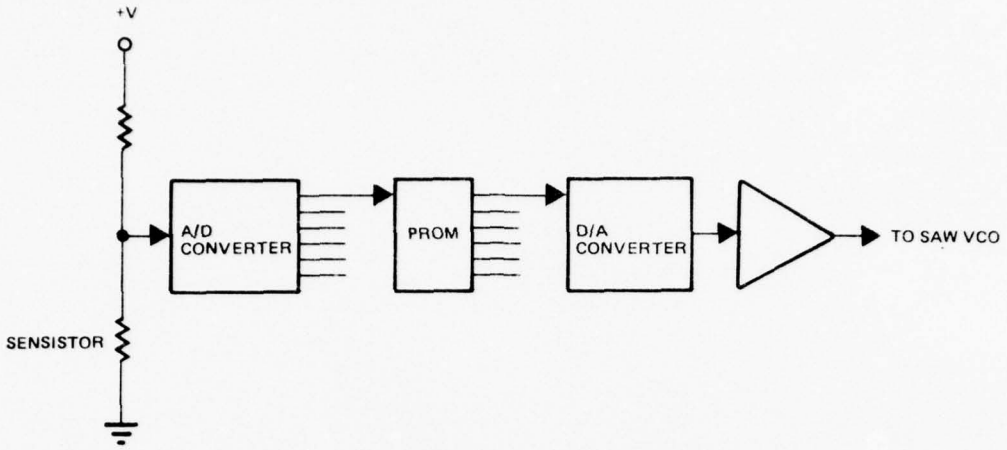

Figure 4-12. Digital Electronically Compensated SAW Oscillator Basic Block Diagram

to its ambient temperature frequency. The PROM is then programmed with this information.

A complete schematic for the circuit is shown in Figure 4-13. To minimize the dc power consumption of the circuit, CMOS A/D and D/A converters are used. (A CMOS PROM was not available.) The digital electronics consumes a total of 450 mW, 400 mW by the TTL PROM. For applications which do not allow the use of CMOS, the circuit can easily be modified to use TTL logic. If low dc power consumption is a requirement, all of the circuitry except the output latch of the D/A may be strobed at a low duty cycle. Using this technique, the oscillator frequency can be corrected periodically while maintaining a low average dc power consumption.

A photograph of the complete oscillator is shown in Figure 4-14. The overall size is 5 x 2.5 x 1 inches, and the complete oscillator weighs 0.7 pound. Figure 4-15 shows the measured frequency variation of the digital electronic temperature compensated SAW oscillator. The variation is a sawtooth due to the basic nature of the circuit, which corrects the variation of the oscillator in discrete steps. The circuit provides corrections in equal temperature increments, but the basic rate of the oscillator frequency variation increases as the temperature deviates from ambient. Therefore, the frequency error of the compensated oscillator tends to increase on either side of the ambient temperature.

This technique has reduced the basic oscillator output frequency variation over the range of 0 to +180°F from an uncompensated value of $\pm$20 kHz ($\pm$80 ppm) to a compensated value of $\pm$2.5 kHz ($\pm$10 ppm). By applying a final iteration to the programming of the PROM, it should be possible to achieve a temperature stability of $\pm$10 ppm over the full -40 to +180°F range. This represents a significant

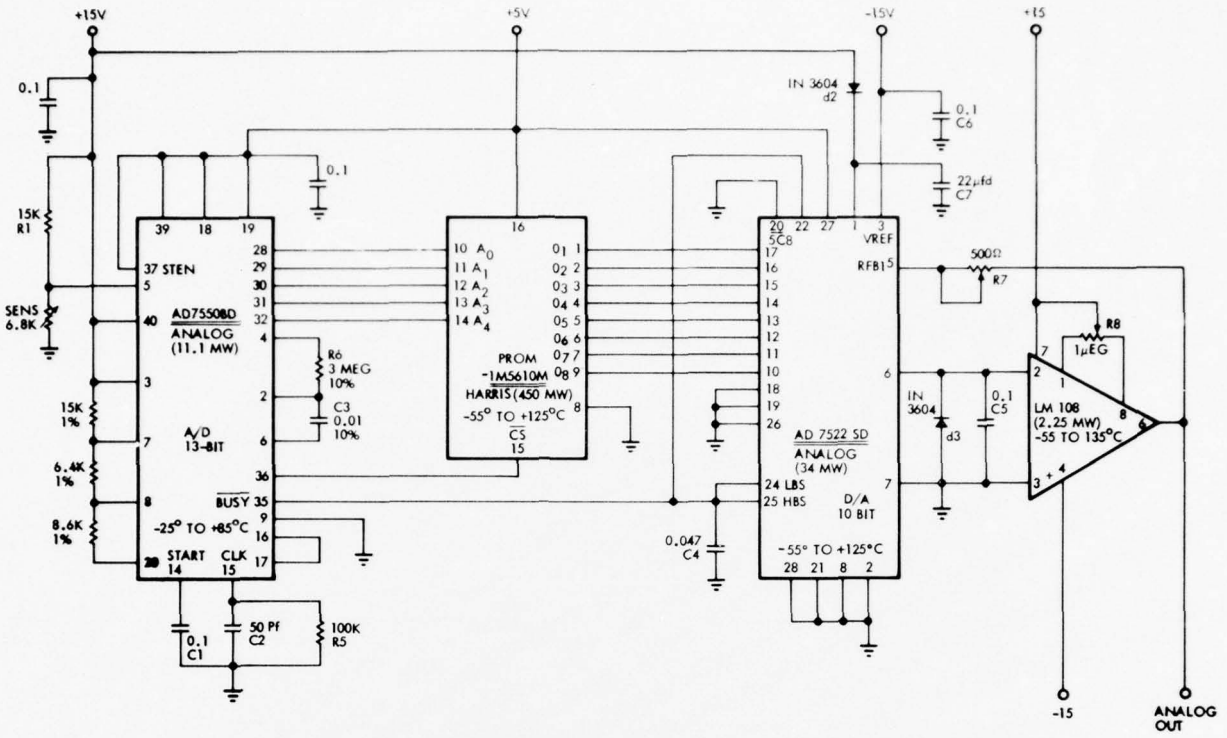

Figure 4-13. Digital Temperature Compensated SAW Oscillator Schematic

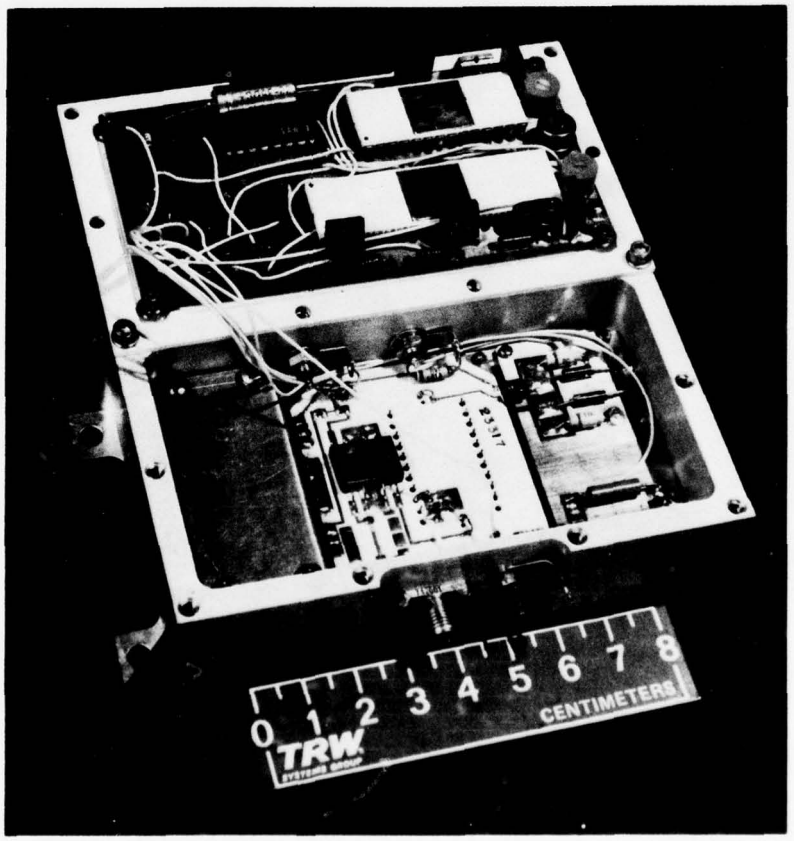

Figure 4-14. 250 MHz Digital Electronically Compensated SAW Oscillator

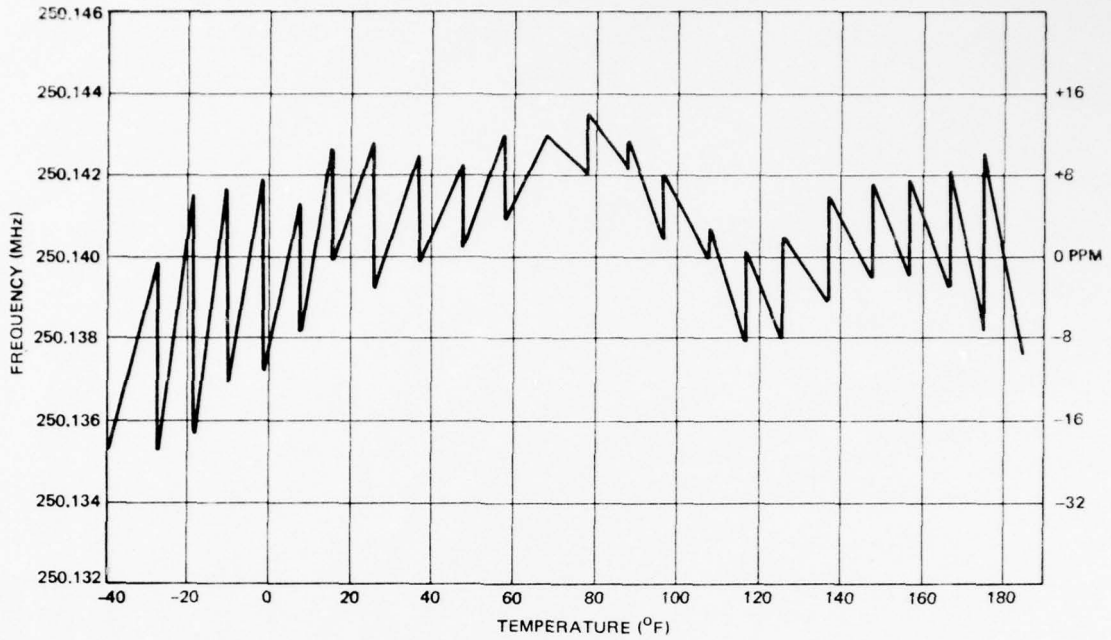

Figure 4-15. 250 MHz Electronically Temperature Compensated SAW Oscillator Temperature Characteristic

improvement in the basic temperature stability of SAW oscillators. Besides temperature compensating the SAW oscillator, the digital circuit makes it possible to perform other complex functions with the SAW oscillator not possible with crystal type frequency sources. For example, by incorporating a digital addition circuit following the PROM, the frequency of the oscillator can be shifted up or down without affecting the temperature compensation. In this manner, the oscillator can be frequency modulated, the frequency aging of the oscillator could be remotely corrected, or the oscillator could be used as a narrowband frequency synthesizer.

The remaining characterization of the oscillator included measuring the output power temperature stability and the oscillator short-term stability. The temperature stability of the oscillator output power is shown in Figure 4-16. The output power variation over the 0 to +100°F range was $\pm$0.15 dB and over the full -40 to +180°F was $\pm$1.3 dB.

The short-term stability of the 250 MHz electronically temperature compensated SAW oscillator was measured in both the time and frequency domains. The results of these tests are shown in Figures 4-17 and 4-18. The total integrated phase noise from 1 kHz to 100 MHz was 0.29° rms. When the lower limit of the integration bandwidth is changed to 10 kHz, the total phase noise drops to 0.06° rms. The time domain short-term stability of the oscillator was measured for averaging times of between 10^{-3} to 10^{1} seconds. The data indicates that a maximum short-term stability of 4×10^{-9} occurs for a 1 second averaging time. The short-term

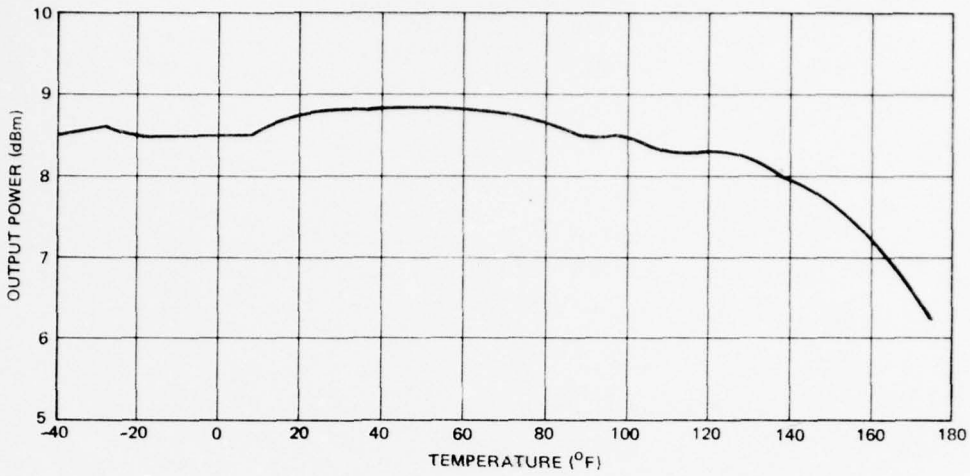

Figure 4-16. 250 MHz Electronically Temperature Compensated SAW Oscillator Output Power Stability

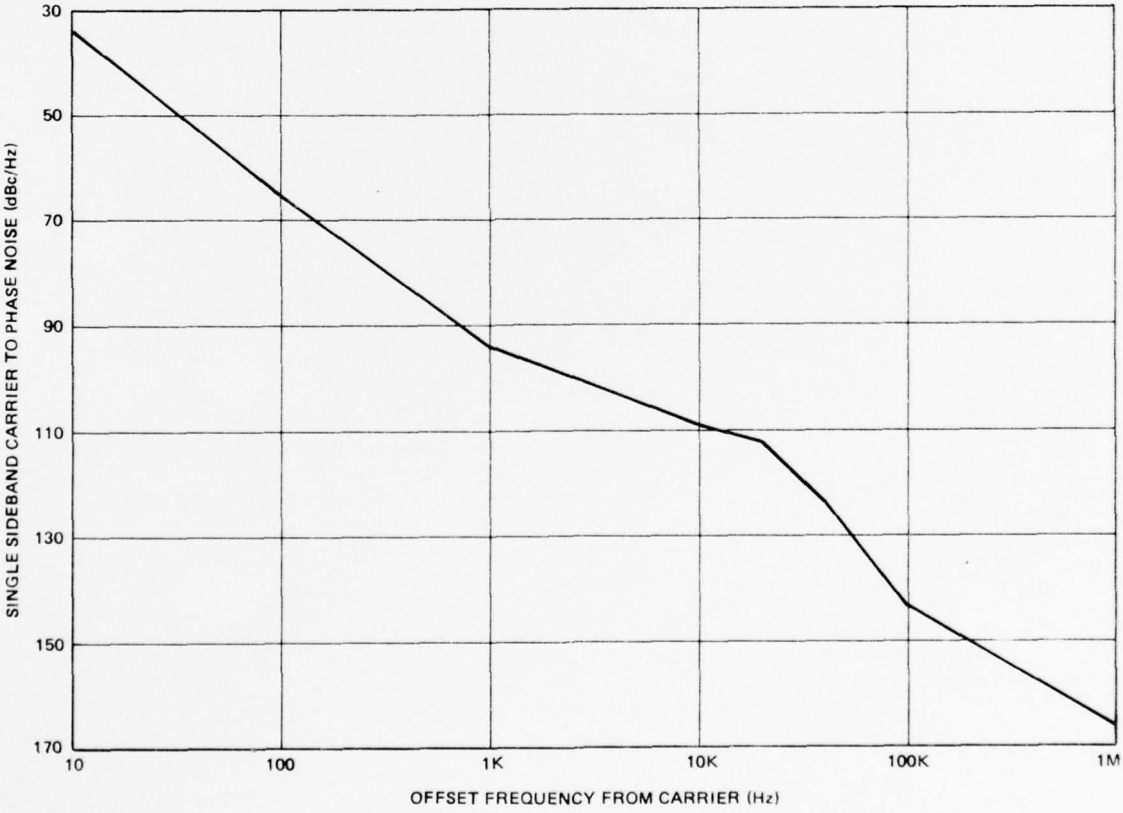

Figure 4-17. Phase Noise Plot of 250 MHz SAW Oscillator With Digital Compensation

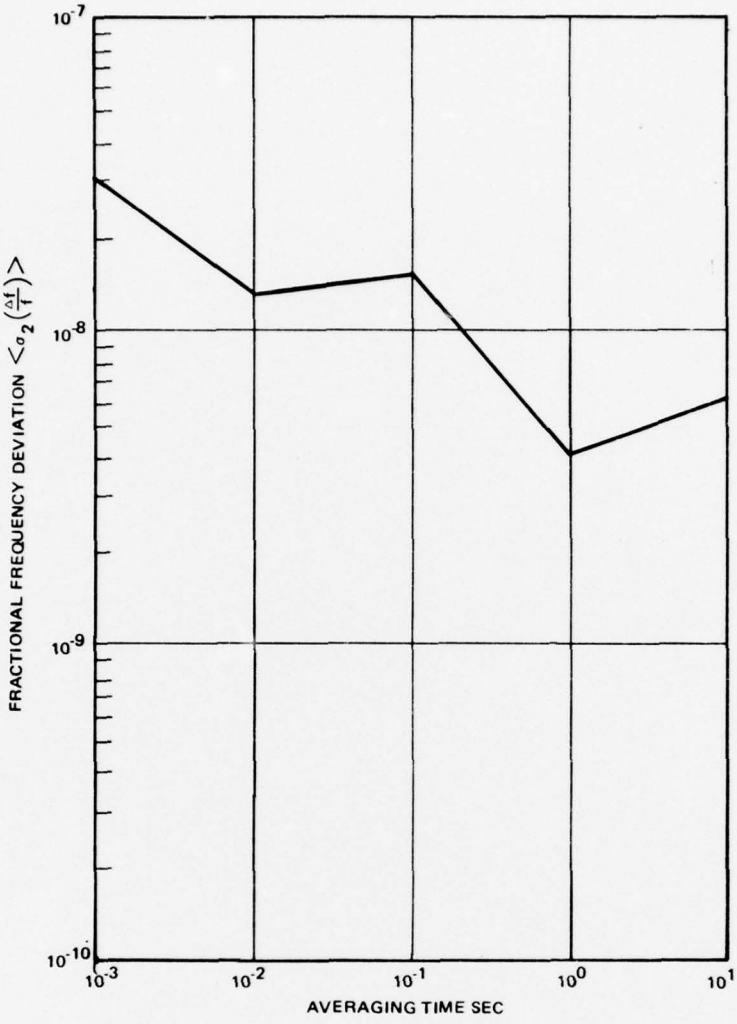

Figure 4-18. 250 MHz Digital Temperature Compensated SAW Oscillator Short Term Stability

stability of the SAW oscillator degrades for averaging times beyond 1 second because from this point on the medium term temperature effects begin to dominate. In the vicinity of ambient temperature, the temperature coefficient of the oscillator is 5×10^{-7} per °F. Therefore, an oscillator temperature shift of just 0.01°F will cause the oscillator frequency to change 1 part in 10^{-9}.

4.3 SAW OSCILLATOR AGING TESTS

The SAW oscillator aging tests are a continuation of the life tests started on a previous contract (N00123-75-C-1182). Four 250 MHz SAW oscillators have been on life test since 17 July 1975. Three months of aging data were accumulated on that contract. During this contract, an additional 9 months of data were recorded for a total of 1 complete year (or over 35,000 oscillator hours) of aging.

4.3.1 Oscillator Fabrication Review

The four identical 250 MHz SAW oscillators were all assembled using techniques which were chosen to optimize the long-term stability of the SAW oscillators. The oscillators consist of a hermetically sealed SAW delay line, a hermetically sealed thin film feedback amplifier, level set attenuator, power divider, and a meander line phase shifter.

The SAW delay lines were hermetically sealed to protect the surface of the SAW crystal from contamination and to mechanically protect the crystal. The total delay through the SAW delay line (and therefore the oscillator frequency) is extremely sensitive to any contamination on the surface of the SAW delay line. For this reason, the processing steps followed to assemble and seal the delay lines were carefully chosen to ensure minimum contamination and stress.

The SAW delay lines and internal matching networks were mounted in a hermetic flatpack on an alumina carrier. Figure 4-19 is a photograph of an assembled delay line prior to sealing. The quartz crystal is attached to the alumina carrier with Dow Corning RTV 6-1104. This material was selected for this application for the following reasons. First, the material exhibits a minimum of outgassing. This is important to prevent contamination of the SAW crystal after it is sealed. Second, the material is flexible and acts as both a mechanical shock absorber for the crystal and absorbs the stresses due to the different thermal coefficient of expansion of the quartz crystal and the alumina carrier. Finally, the material is used to absorb the acoustic waves which reach the edges of the SAW crystal and would otherwise be reflected back to the transducers.

Electrical connections to the transducers are made using ultrasonically bonded aluminum wires. Thermal compression bonding is not used because the SAW crystal would have to be preheated to a high temperature prior to bonding and the possibility of causing crystal microfractures under the bonds. The chip capacitors and hand-wound inductors were attached to the carrier using a silver filled conductive epoxy also selected for minimum outgassing. The components are not soldered because of the possibility of flux or solder contaminating the delay line. Finally the entire carrier was mounted in the flatpack using the same conductive epoxy that was used to attach the chip components. The input and output connections were made by wire bonding from the carrier pads to the leads of the package.

The processing steps followed to seal the delay lines were carefully chosen to ensure that the delay lines were kept as clean and as dry as possible. The crystals were first cleaned with a fine camel hair brush and acetone. They were next blown dry with dry nitrogen to clean any dust particles from the packages. The crystals were then vacuum baked for 24 hours at 150°F to further dry the quartz crystal and to minimize the trapped gasses in the RTV and epoxy. Following

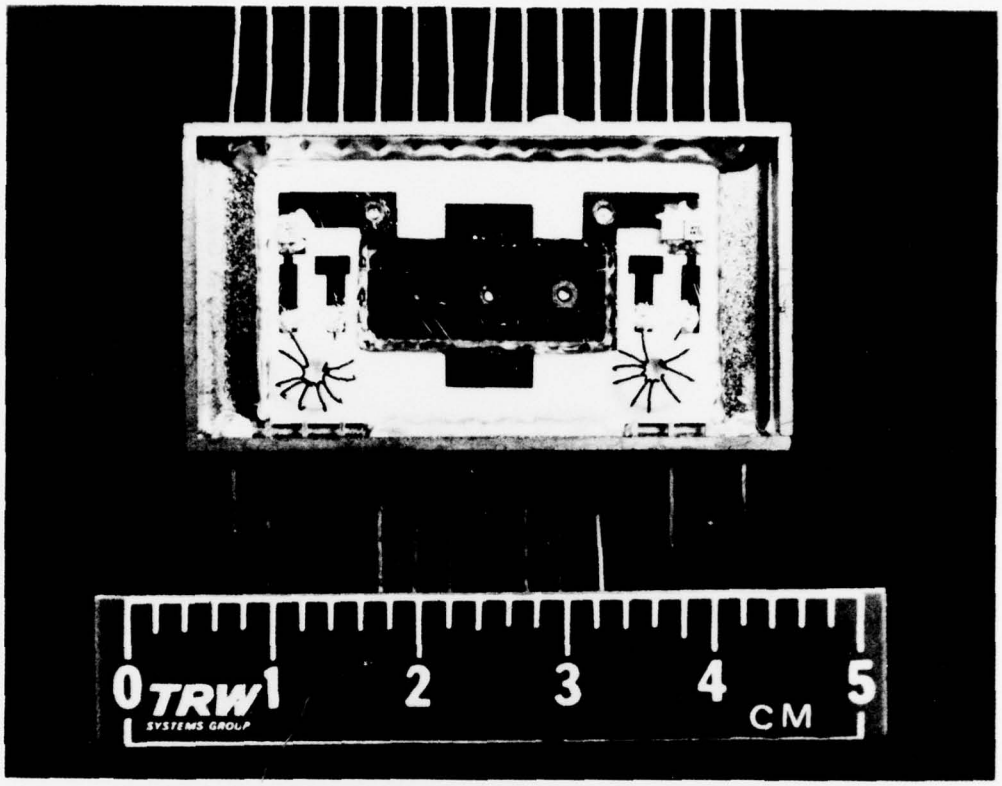

Figure 4-19. 250 MHz SAW Relay Line

the vacuum bake, the packages were stored in dry nitrogen to clean any dust particles from the packages. The crystals were then vacuum baked for 24 hours at 150°F to further dry the quartz crystal and to minimize the trapped gasses in the RTV and epoxy. Following the vacuum bake, the packages were stored in dry nitrogen until they were hermetically sealed. Finally, the sealed packages were both fine and gross leak checked to confirm that the packaged delay lines were hermetically sealed. Following the sealing process, the input and output return loss and the insertion loss of the delay lines were rechecked. In general, no significant degradation was measured due to the sealing process.

The alignment process for the oscillators is very simple. The first step is to determine the difference between the delay line insertion loss and the linear amplifier gain. The attenuator in the loop is then set so that there is approximately 3 dB of excess gain in the loop. The amount of excess linear amplifier gain determines the level of saturation in the amplifier when the loop is oscillating, and affects the noise performance of the oscillator.

The second step in aligning the oscillators is to adjust the total loop phase shift. The total loop phase shift (or oscillator frequency) was fine tuned by a

meander line phase shifter. The total length of the line is varied by interconnecting lines of different lengths. Relative phase shifts of up to 360° in 2.5° increments could be selected at 250 MHz. A variable capacitor network could have been used to perform this function, but the temperature and long-term stability of the oscillator would have been degraded.

The oscillator is first tested with a nominal amount of phase shift. The output frequency is then fine tuned either up or down to the exact desired frequency by either decreasing or increasing the total length of the meander line. Using this technique, the oscillators can be adjusted over a range of approximately ±100 kHz with a resolution of approximately ±5 kHz. Table 4-2 summarizes the data for the four oscillators following their initial alignment. In each case, the output frequencies of the oscillators were adjusted to correspond to the frequency of minimum insertion loss of the SAW delay used in the oscillator.

Table 4-2. SAW Oscillator Performance Summary

Serial No.	f_o (MHz)	P_{out} (dBm)	Bias Current at +15 V (mA)
SN23311	249.699	9.9	67
SN23313	249.757	10.2	69
SN23315	249.704	9.2	66
SN23316	249.784	10.0	68

4.3.2 Life Test Results

The aging test of the four 250 MHz SAW oscillators was started on 17 July 1975. All four oscillators were mounted on a common baseplate in a thermally isolated environment and temperature stabilized at 92°F. The life tests were conducted in two different phases. First, the oscillators were continuously tested for a total of 12 months; this was followed by a 3 month bias cycling test. The following summarizes the results of these tests.

1 Year Life Tests

The oscillators were first subjected to a 168 hour burn-in period. This type of burn-in is standard for high reliability components and is done for two reasons: to screen the semiconductors for early catastrophic failures and to separate the short-term burn-in effects of the oscillator performance from the long-term aging effects. During the burn-in period, the oscillator output powers varied from -1 to +0.4 dB and the output frequencies varied from +1.8 to -2.8 ppm.

During the aging test, the oscillator baseplate temperature was continuously monitored. The data was recorded at the same time early each morning. During the period of the test, the baseplate temperature of the oscillators varied less than $\pm$0.5°F. Temperature changes of this magnitude will result in oscillator frequency variations of less than $\pm$0.2 ppm. For this reason, it was not necessary to compensate the oscillator frequency data due to ambient temperature changes.

The frequency aging rates for the four oscillators during the 1 year of continuous life tests are summarized in Table 4-3. The actual aging curves are shown in Figure 4-20. The average aging rate for the four oscillators over the 1 year period was -21 ppm per year. The frequency aging of the oscillators is exponential as evidenced by the decreasing aging rates. An additional 18 weeks of aging data has been collected beyond the 1 year period. During this 18 week period, the average aging rate for the four oscillators dropped to less than -6 ppm per year.

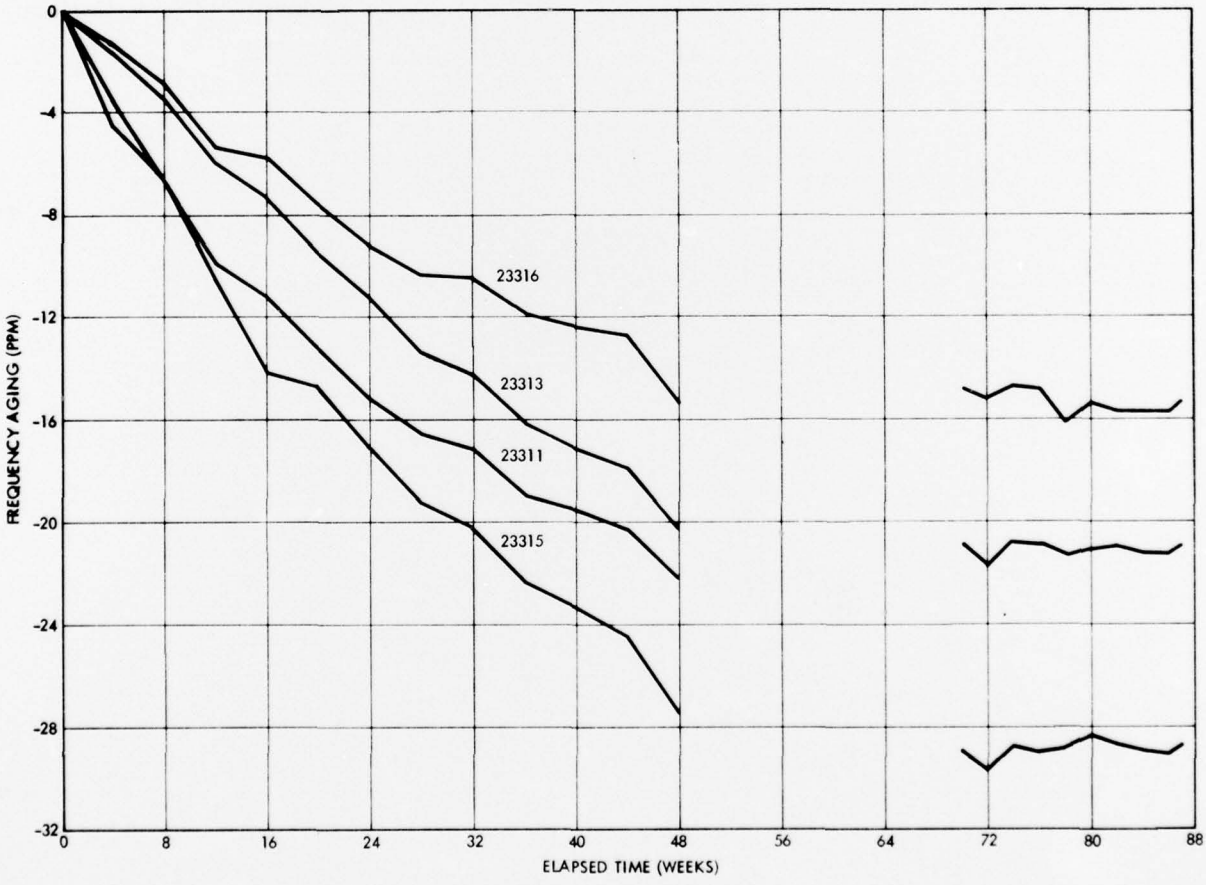

Figure 4-20. Aging Rates for Four 250 MHz SAW Oscillators

Table 4-3. SAW Oscillator Aging Summary

Serial No.	Aging Rate PPM per Year				
	First 3 Month Period	Second 3 Month Period	Third 3 Month Period	Fourth 3 Month Period	Total for 1 Year
23316	-4.4	-19.6	-9.2	-6.0	-9.8
23313	-13.2	-26.0	-19.2	-11.2	-17.4
23311	-44.8	-26.8	-15.2	-10.8	-24.4
23315	-57.6	-34	-20.4	-17.6	-32.4
Average	-30.0	-26.6	-16.0	-11.4	-21.0

Three Month Bias Cycling Tests

The purpose of these tests was to isolate the aging effects in the SAW delay line from those in the remaining loop electronics. Based on existing data for electronic components, the aging rate of the oscillators should be a positive function of temperature; that is, a decrease in temperature should bring about a corresponding decrease in aging rate. The two methods of evaluating the aging characteristics of the SAW oscillators considered were to cycle the oscillator bias on and off and to elevate the oscillator temperature above the baseline value of 92°F.

The first technique was chosen because it offered the potential of separating the aging rate of the delay line from that of the remaining loop electronics. The aging rate of the amplifier alone should decrease when the bias is off whereas the aging rate of the SAW delay line should be independent of amplifier bias. The test was performed by separating the four oscillators into two pairs. The control pair of oscillators was operated continuously. The bias on the other pair was turned off and only turned on long enough once each week (approximately 5 minutes) to measure the oscillator frequency. When the oscillator bias is turned off, the temperature of the delay line drops ≈ 10°F due to the overall reduction in dc power dissipation and hence oscillator baseplate temperature. The junction temperature of the transistors in the loop amplifier, however, is reduced by ≈ 100°F due to the thermal resistance of the chip transistors. If the two unbiased oscillators had shown a reduction in aging rate compared to the remaining pair of biased oscillators, the results of the test would have suggested that the amplifiers were dominating the oscillator aging, whereas if no significant change in the aging rate had occurred, it would suggest that the delay lines were dominant.

The results of the 13 weeks of bias cycling tests are shown in Figure 4-21. The average aging rate for the continuously-biased pair was 5.5 ppm per year vs

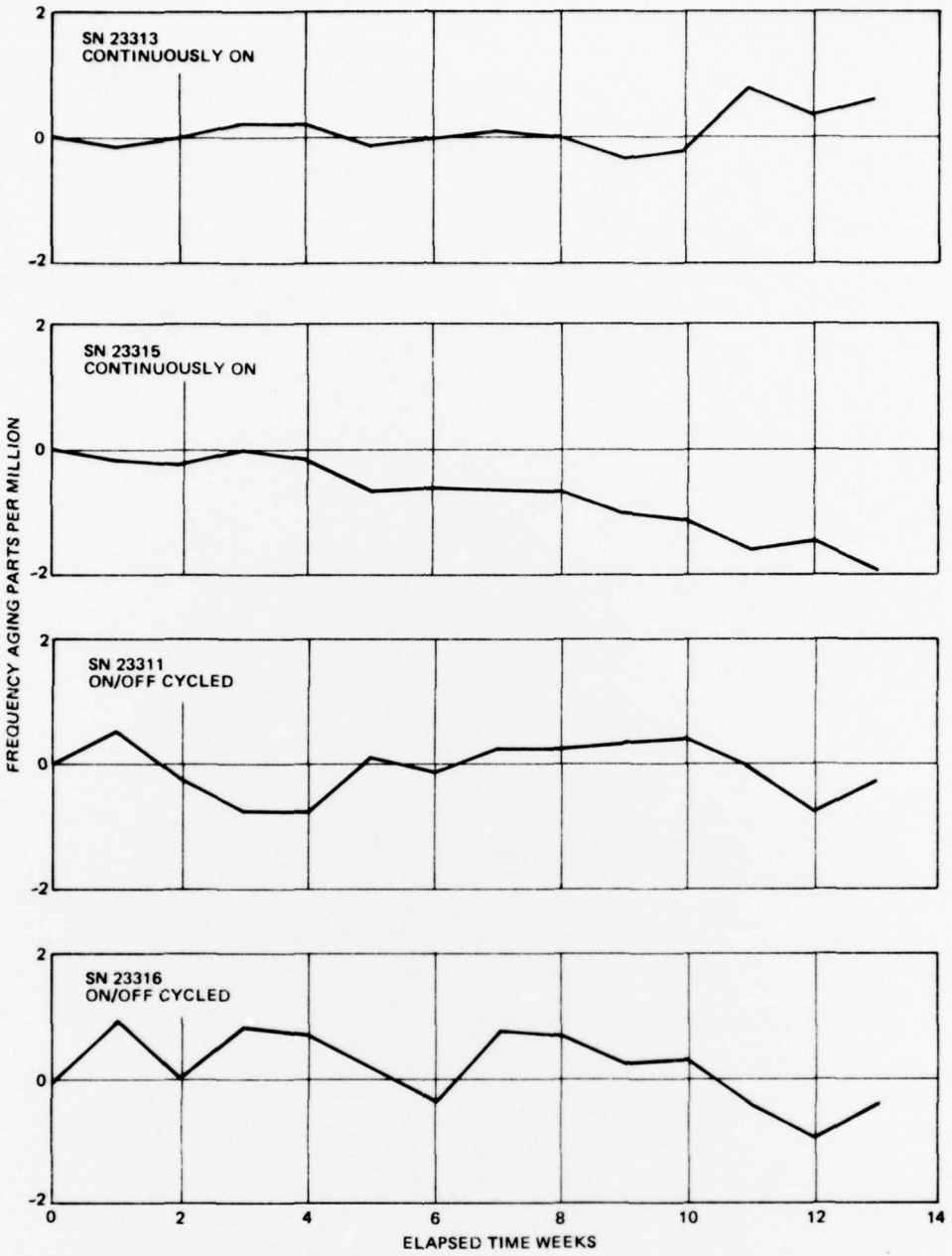

Figure 4-21. SAW Oscillator Bias Cycling Aging Results

6.0 ppm per year for the on/off biased pair. The slightly higher aging rate of the cycled pair is most likely due to thermal transients in the oscillators during turn-on. Based on the assumptions made when these tests were started concerning aging mechanisms and that there was no significant difference in the aging rate between the two pairs of oscillators, it appears that the SAW delay lines dominated the oscillator aging rate. Based on these results, future investigation should focus on identifying aging mechanisms in the SAW delay lines.

4.4 250 MHz AND 500 MHz DELIVERABLE OSCILLATORS

In addition to the 250 MHz electronically temperature compensated and the 1 GHz SAW oscillators, two additional SAW oscillators, one operating at 250 MHz and one at 500 MHz, were delivered to NELC. The following sections describe the performance of these two oscillators.

4.4.1 250 MHz SAW Oscillator

One of the four 250 MHz SAW oscillators (No. 23311) that was on life test was delivered to NELC. Prior to delivery, this oscillator was continuously operated for a period of 18 months (approximately 13,000 hours). The oscillator consists of a hermetically sealed SAW delay line, a loop amplifier substrate, and a meander line phase shifter substrate. All of the components were mounted in a machined aluminum chassis. A photograph of the oscillator prior to sealing of the SAW delay line is shown in Figure 4-22. Table 4-4 summarizes the performance of the oscillator.

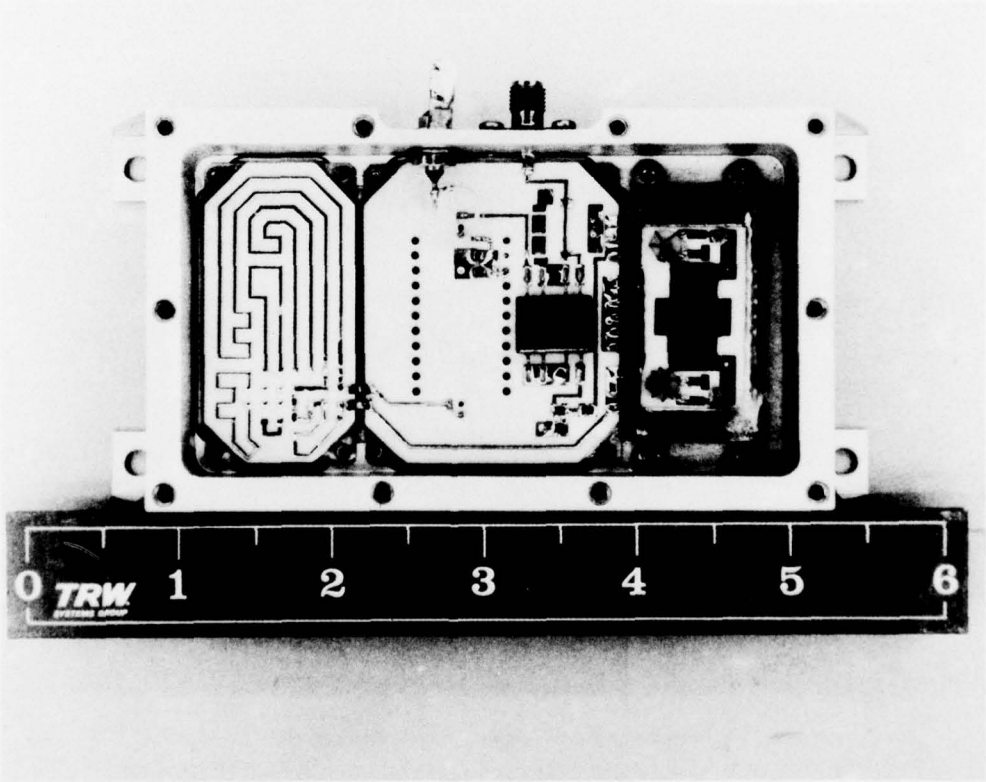

Figure 4-22. 250 MHz SAW Oscillator

Table 4-4. 250 MHz SAW Oscillator Performance

Parameter	Performance
Frequency	249.690 MHz
Output power	+9.5 dBm
Temperature stability -40 to +180°F	$\Delta f = \pm 0.01\%$
	Δpower = $\pm$0.5 dB
Phase noise	-124 dBc/Hz at 10 kHz

The amplifier and meander line phase shifter were both fabricated on alumina microstrip circuits. The amplifier is contained in a hermetic 22-pin package. The package is mounted on the ground plane side of the substrate using conductive epoxy. The power divider, attenuator, bias bypass capacitors, and interconnecting circuitry are all on the top side of the substrate. The meander line substrate is simply a number of 50 ohm lines of various lengths. The different lines are then interconnected using ribbons to select the required phase shift. Both substrates are mounted on Kovar carriers which are attached to the oscillator chassis with screws. Spring finger frames under each substrate ensure a good ground contact between the substrate ground plane and the chassis.

A complete characterization of the oscillator, including output power and frequency as a function of temperature and phase noise, was performed. The temperature test results are shown in Figures 4-23 and 4-24. The frequency variation over the -60 to +100°F range was $\pm$0.011% and the output power variation was $\pm$0.5 dB. The phase noise plot for the oscillator is shown in Figure 4-25. The total integrated phase noise from 10 kHz to 1 GHz was 0.06° rms. The high level of performance, particularly phase noise, demonstrates that SAW oscillators are a viable replacement for bulk-crystal oscillator/multiplier chain frequency sources.

4.4.2 500 MHz SAW Oscillator

The fourth deliverable SAW oscillator operates at a frequency of 494 MHz. This oscillator was assembled using the same basic techniques applied to the fabrication of the 250 MHz oscillator. A meander line phase shifter was not required for this oscillator and the oscillator was therefore packaged in a smaller housing than was required for the 250 MHz oscillator. Table 4-5 summarizes its characteristics.

Table 4-5. 500 MHz SAW Oscillator Performance

Parameter	Performance
Frequency	494.330 MHz
Output power	+9.2 dBm
Temperature stability -40 to +180°F	$\Delta f = \pm 0.012\%$
	Δpower = $\pm$0.3 dB
Short term stability	5×10^{-10} for 100 msec
Phase noise	-120 dBc/Hz at 10 kHz

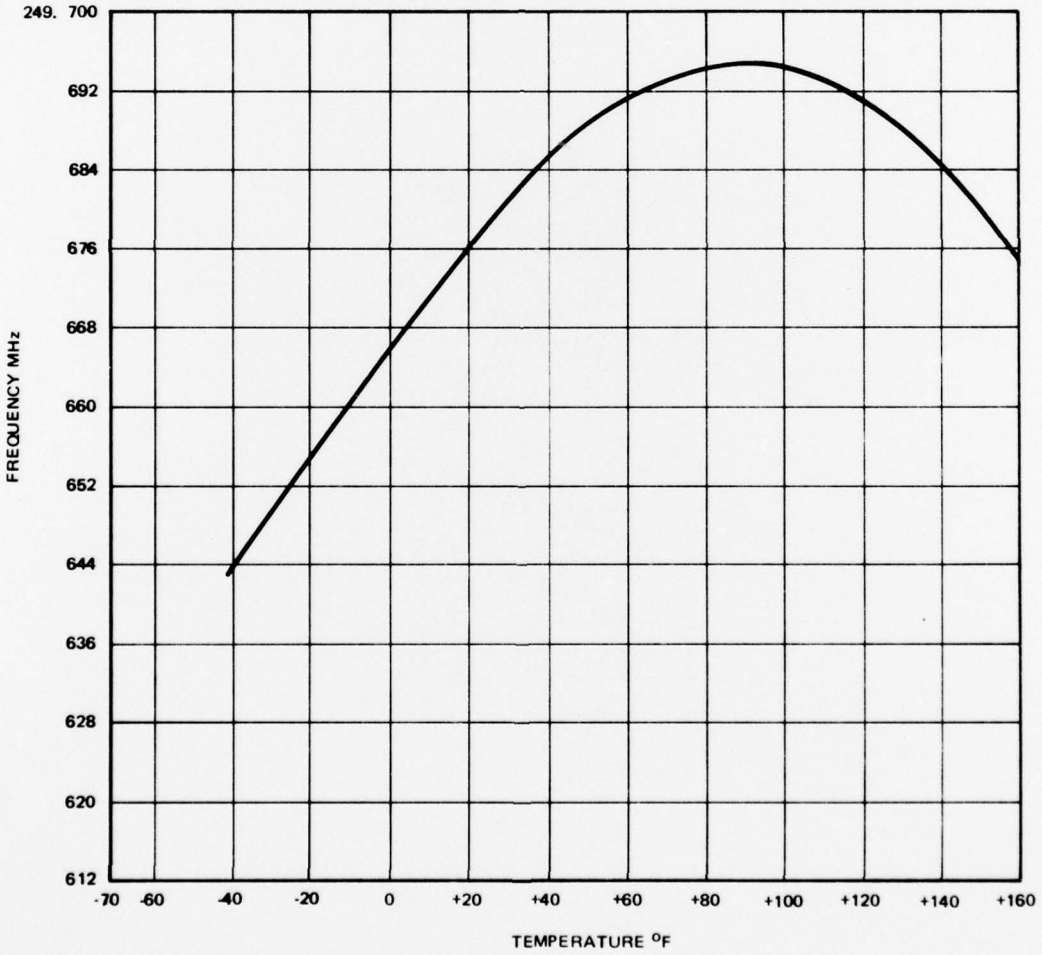

Figure 4-23. 250 MHz SAW Oscillator Frequency at Function of Temperature

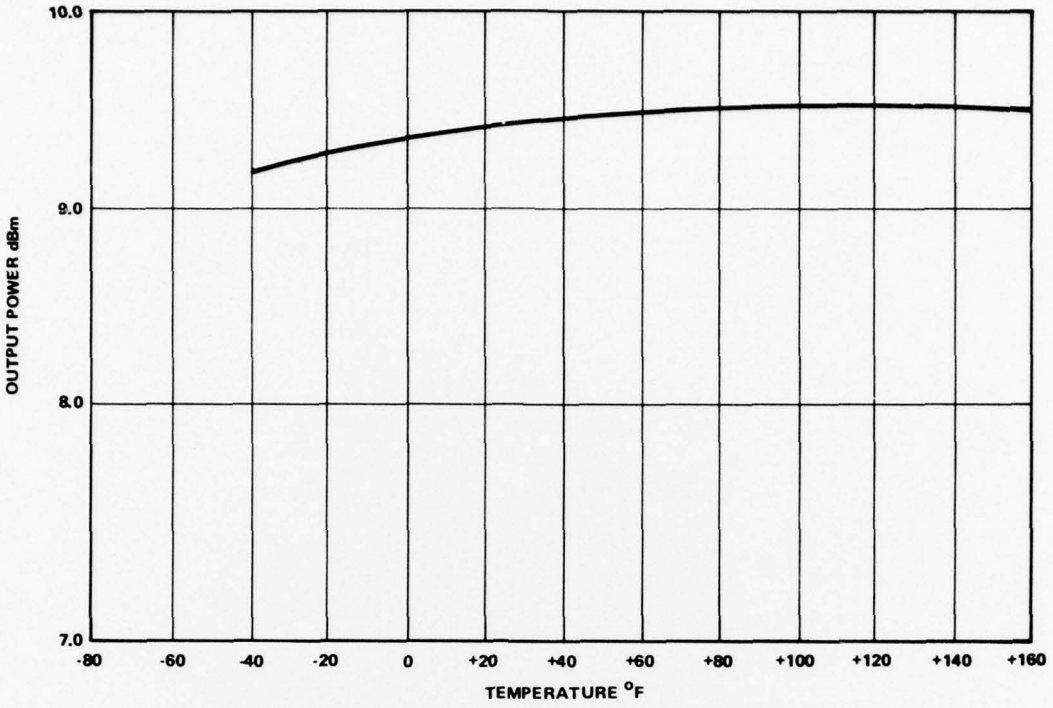

Figure 4-24. 250 MHz SAW Oscillator Output Power vs Temperature

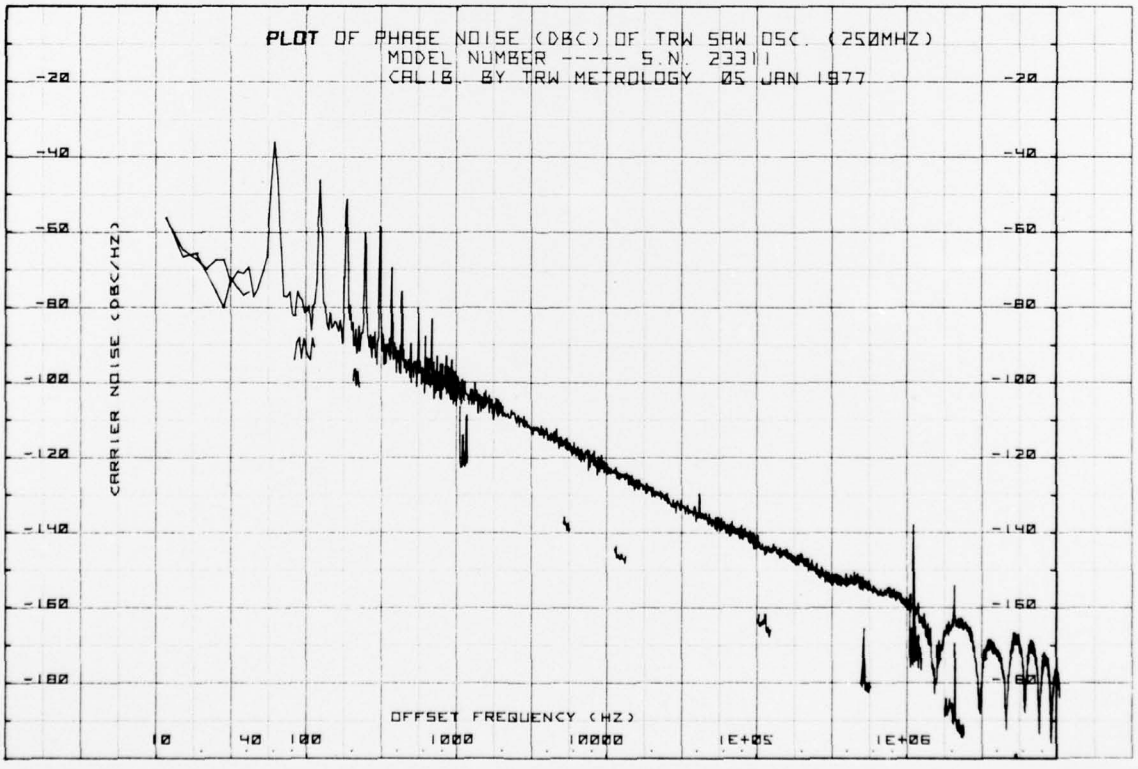

Figure 4-25. 250 MHz SAW Oscillator Phase Noise Measurement

A complete characterization of the oscillator was performed. Measurements included output power and frequency as a function of temperature and short-term stability in the time and frequency domains. The oscillator frequency and power as a function of temperature are shown in Figures 4-26 and 4-27. The frequency variation over the -60 to +100°F temperature range was $\pm$25 ppm ($\pm$0.025%) and the variation was $\pm$0.05% over the full -80 to +200°F range. The oscillator output variation was only $\pm$0.4 dB over the full -60 to +200°F range. The oscillator exhibited this high level of stability because the oscillator power is determined by the saturation in the loop amplifier.

The frequency domain phase noise and the time domain short-term stability of the oscillator were both measured. The phase noise (Figure 4-28) followed a $1/f^3$ slope for offset frequencies between 10 to 100 MHz and $1/f^2$ beyond 100 Hz. The phase noise reached a final value of -160 dB/Hz at an offset frequency of 1 MHz. The total integrated phase noise from 10 kHz to 1 GHz was 0.07° rms. The short-term stability for the oscillator is shown in Figure 4-29. An optimum value of 5×10^{-10} was achieved at a 100 msec gate time.

Previous measurements of the time domain short-term stability of several different 250 and 500 MHz SAW oscillators indicated that a typical maximum short-term stability of 1×10^{-9} is achieved for averaging times of between 0.1 and 1 second. The short-term stability of the SAW oscillator degrades for averaging times beyond 1 second because from this point on the medium-term (temperature) stability begins to dominate. In the vicinity of ambient temperature, the temperature coefficient of the 500 MHz oscillator is about 1×10^{-6} per °F. Therefore, an oscillator temperature shift of just 0.001°F will cause the oscillator frequency to change 1 part in 10^{-9}, thus creating a limiting value for short-term stability unless very elaborate temperature stabilization techniques are employed.

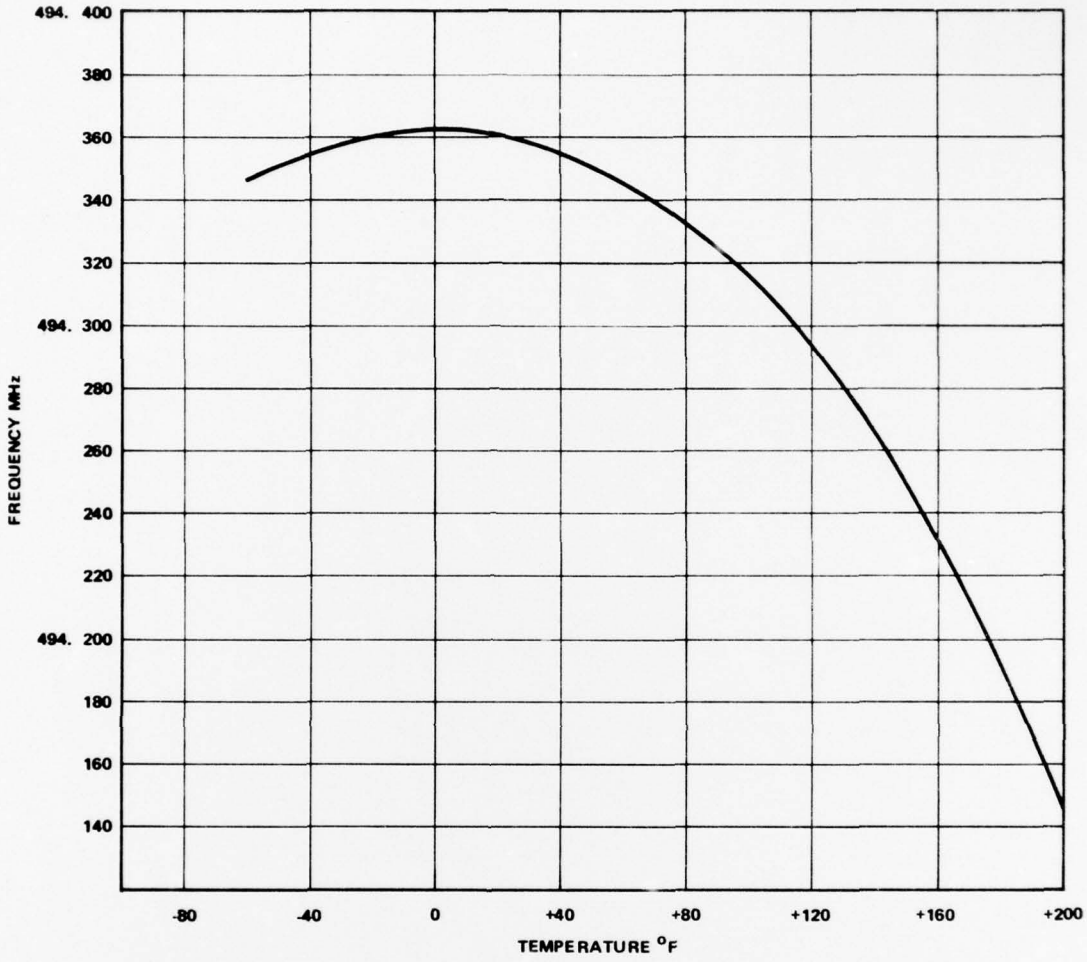

Figure 4-26. 500 MHz SAW Output Frequency as a Function of Baseplate Temperature

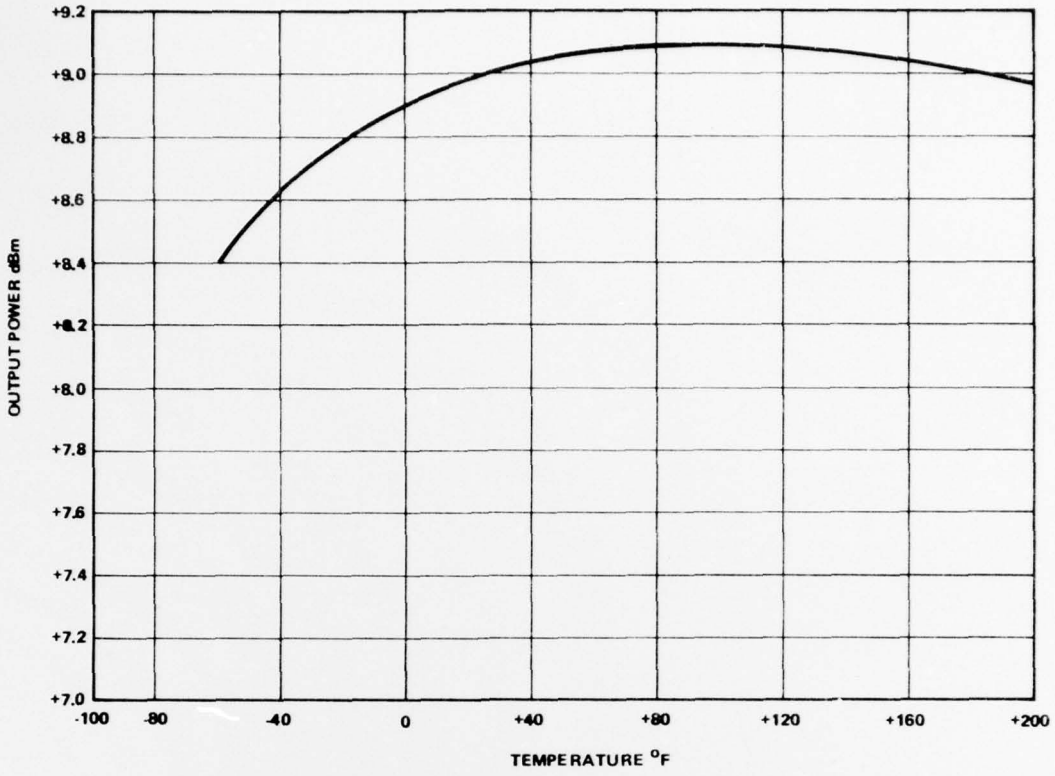

Figure 4-27. 500 MHz SAW Oscillator Output Power as a Function of Temperature

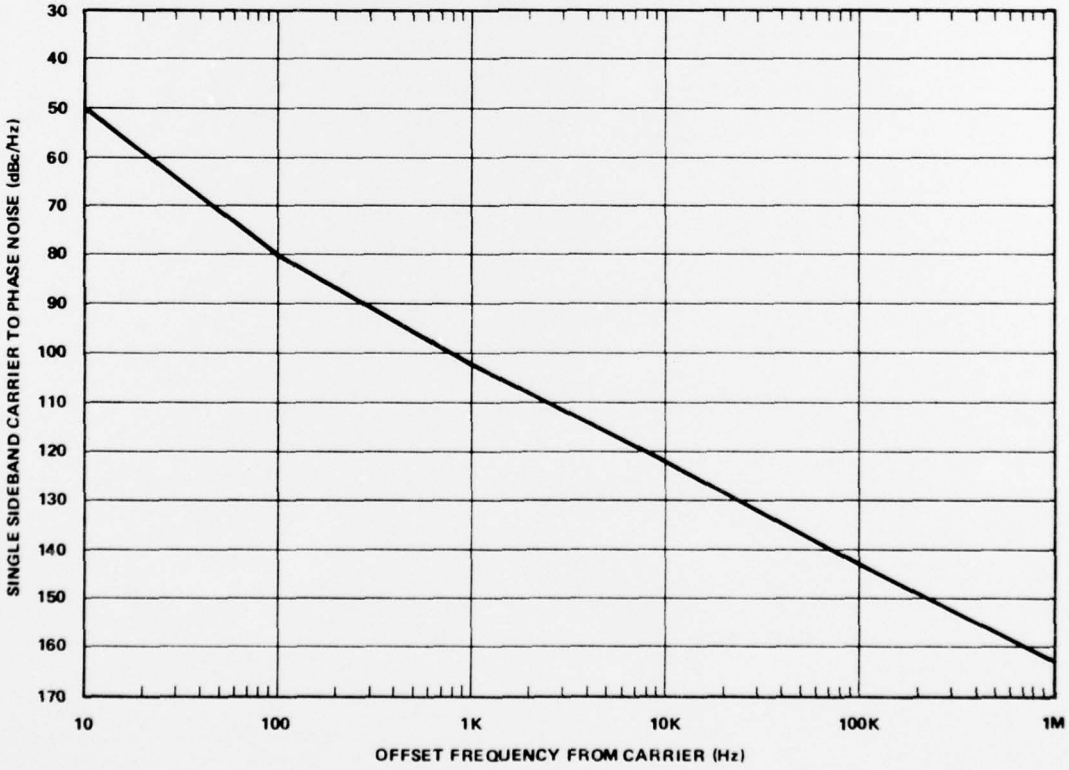

Figure 4-28. Phase Noise Plot of 494 MHz SAW Oscillator

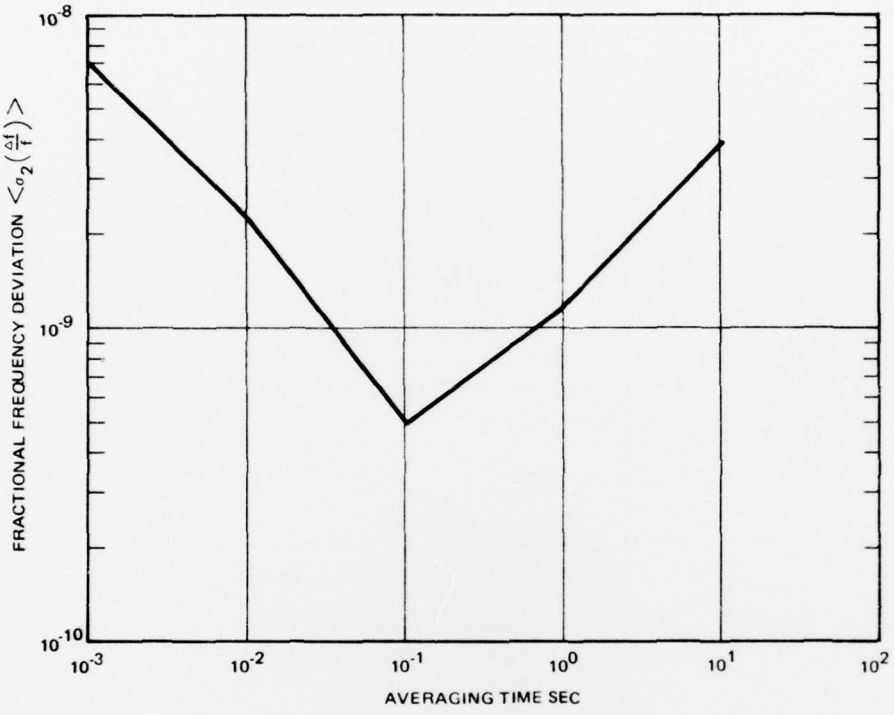

Figure 4-29. 494 MHz SAW Oscillator Short Term Stability